https://doi.org/10.5194/egusphere-2026-2710
Preprint. Discussion started: 4 June 2026

Spatial differentiation of carbon-control structures in urban coastal ecosystems under nutrient enrichment

Kohei Kawahito[1], Daichi Okada[1,2], Akio Sohma[1,2]

[1] Graduate School of Engineering, Osaka Metropolitan University, Sumiyoshi-ku, Osaka 558-8585, Japan;
[2] Graduate School of Engineering, Osaka City University, Sumiyoshi-ku, Osaka 558-8585, Japan;

Correspondence to: Akio Sohma (sohma@omu.ac.jp)

Abstract. Urban coastal ecosystems, which are strongly influenced by human activities and elevated nutrient inputs, can contribute to climate-change mitigation through carbon uptake, fixation, and storage. However, it remains unclear how the underlying carbon-control structures governing these functions respond to nutrient enrichment, owing to the interactions of multiple biogeochemical processes across pelagic and benthic systems. In this study, we applied the benthic–pelagic coupled ecosystem model EMAGIN-B.C. ver. 2 to Tokyo Bay to examine how nutrient loading influences carbon cycling in urban coastal environments. To interpret these responses mechanistically, carbon cycling was organised into three paired flux balances representing carbon uptake (A/R), carbon fixation (F/U), and carbon storage (S/D). These functional pairs were analysed within a conceptual framework of a Dual Carbon Loop consisting of organic and carbonate pathways. Model simulations demonstrate that increased nutrient loading enhances atmospheric CO_2 uptake and pelagic carbon fixation. However, the dominant mechanisms controlling carbon cycling differ substantially across regions. In the estuarine region, nutrient enrichment amplified pelagic primary production, resulting in simultaneous increases in carbon uptake, fixation, and organic carbon burial. In the central bay, production and remineralization are intensified in tandem, indicating strong internal coupling of carbon fluxes. In contrast, tidal flats exhibited a transformation-dominated response wherein externally supplied organic matter was rapidly processed by benthic communities, thereby limiting net pelagic fixation while maintaining relatively stable carbonate storage and producing a system characterised more by transport, transformation, and redistribution than by new production. These contrasting responses indicate that identical nutrient forcing can produce distinct carbon-cycling behaviours depending on the regional ecosystem structure. We interpret these patterns as spatial differentiation of carbon-control structures governed by the relative balance of opposing carbon fluxes within the Dual Carbon Loop system. The proposed framework provides a mechanistic basis for understanding how nutrient management influences climate-mitigation functions in urban coastal ecosystems and offers a perspective for analysing shallow, nutrient-enriched coastal systems characterised by strong benthic–pelagic biogeochemical coupling.

https://doi.org/10.5194/egusphere-2026-2710
Preprint. Discussion started: 4 June 2026

1 Introduction

According to the Sixth Assessment Report of the IPCC (IPCC, 2021), under the SSP5-8.5 scenario representing the highest greenhouse gas emissions, the global mean surface temperature is projected to increase by up to 5.7 °C during 2081–2100 relative to the 1850–1900 baseline. Therefore, reducing greenhouse gas emissions—particularly CO_2—remains an urgent global challenge. In this context, the ocean functions as a major sink and storage reservoir for atmospheric CO_2 (Archer and Brovkin, 2008; Falkowski et al., 2000; Solomon, 2007; McLeod et al., 2011). Oceanic carbon storage is governed by a sequence of coupled processes comprising (1) uptake of atmospheric CO_2 into seawater via air–sea CO_2 fluxes (carbon uptake), (2) fixation of dissolved inorganic carbon (DIC) into biological biomass through photosynthesis and shell formation (carbon fixation), and (3) burial of fixed carbon into deeper sediment layers (carbon storage) (Sohma et al., 2018) (**Fig. 1**). Urban coastal areas with high biological productivity are considered to have a significant potential to mitigate climate change through these processes of carbon uptake, fixation, and storage (Nellemann et al., 2009). Studies on carbon fixation and storage in coastal ecosystems, including blue-carbon ecosystems, have progressed worldwide (Alongi, 2016; Chen, 2013; Chmura, 2003; Donato et al., 2011; Fourqurean et al., 2012; Frankignoulle et al., 1998; Kubo and Kanda, 2017; Kuwae et al., 2016; Murdiyarso et al., 2015). Nutrients such as inorganic nitrogen and phosphorus flowing into urban coastal areas alter biological production, particularly primary production, thereby influencing carbon uptake, fixation, and storage. A large portion of these nutrients originates from anthropogenic sources; therefore, their inflow loads are manageable. In Japan, nutrient loads to enclosed coastal seas—such as Tokyo Bay, Ise–Mikawa Bay, Osaka Bay, and Seto Inland Sea—have been reduced through wastewater discharge regulations since the 1970s and nutrient control policies since the 2000s (Ministry of the Environment, 2011; Ogura and Takada, 1995; International EMECS Centre, 2008). In recent years, seasonal control of advanced wastewater treatment has been attempted as a measure to address oligotrophication (Japan Fisheries Engineering Association, 2024; Nishijima, 2019; Okamoto, 2021; Ministry of Land, Infrastructure, Transport and Tourism, 2023). Consequently, nutrient management is being reconsidered not only as a water-quality policy but also as a component of climate-change mitigation strategies. However, the influence of nutrient loading on climate-mitigation functions in coastal ecosystems is not straightforward. Increased nutrient input may enhance primary production and stimulate air–sea CO_2 uptake through DIC consumption. Nevertheless, these processes strongly depend on the dynamics of the carbonate equilibrium system (DIC, total alkalinity (TA), pH, and pCO_2) (Dickson et al., 2007; Hoffert et al., 1979). Furthermore, the carbonate system itself is dynamically regulated by biological metabolism, chemical reactions, and physical mixing processes (Yates et al., 2007; Fennel and Wilkin, 2009; Turi et al., 2014; Thomas et al., 2009; Donato et al., 2011).

In addition, enhanced organic matter sedimentation associated with increased production may induce anaerobic conditions in sediments (Canfield, 1994; Jessen et al., 2017), thereby altering mineralization rates (Bastviken et al., 2003; Kristensen and Holmer, 2001; Hedges and Keil, 1995; Andersen, 1996). Such changes may lead to hypoxia-induced mortality of benthic fauna and variations in shell formation, potentially exerting both positive and negative effects on carbon fixation and storage.

https://doi.org/10.5194/egusphere-2026-2710
Preprint. Discussion started: 4 June 2026

Moreover, $CaCO_3$ formation consumes TA and lowers pH, thereby altering pCO_2 and influencing air–sea CO_2 exchange (Thomsen et al., 2018; Zhou et al., 2024). Overall, the response of climate-mitigation functions to nutrient inputs represents a complex system governed by the coupling among carbonate chemistry, ecosystem processes, and biogeochemical dynamics across the atmosphere–pelagic–benthic system. Importantly, these coupling strengths and dominant processes may vary spatially depending on regional characteristics. For example, in estuarine areas, photosynthesis may intensify under high-nutrient conditions, while river water characterised by low pH and high pCO_2 (Ikuta et al., 2005; Ando et al., 1992) may enhance CO_2 release to the atmosphere. In tidal-flat environments, repeated exposure and inundation can enhance benthic metabolism, and alkalinity consumption associated with shell formation may strongly influence the carbonate equilibrium. In central bay areas, differences in physical mixing and water residence time may lead to alternative balances between production and remineralization. Therefore, climate-mitigation functions in urban coastal environments cannot be interpreted as a single, uniform response to nutrient inputs. Instead, the governing carbon processes may spatially differentiate depending on regional environmental characteristics such as hydrodynamic conditions, benthic–pelagic coupling, and ecosystem structure. In this study, we applied the benthic–pelagic coupled ecosystem model EMAGIN-B.C. (Sohma et al., 2018) to Tokyo Bay to examine how nutrient loading influences carbon uptake, fixation, and storage in contrasting coastal environments. To interpret these responses mechanistically, carbon cycling processes were organised into three paired flux balances: carbon uptake (A/R), carbon fixation (F/U), and carbon storage (S/D). These functional pairs were analysed within a conceptual framework of a Dual Carbon Loop consisting of organic and carbonate pathways.

Using this framework, we compared the responses of carbon cycling across three representative regions of Tokyo Bay—estuarine region, central bay, and tidal flats. By examining the relative dominance of opposing carbon fluxes in each region, we identified distinct carbon-control structures governing carbon uptake, fixation, and storage. The objective of this study is to elucidate the spatial differentiation of carbon-control structures in urban coastal ecosystems under nutrient enrichment.

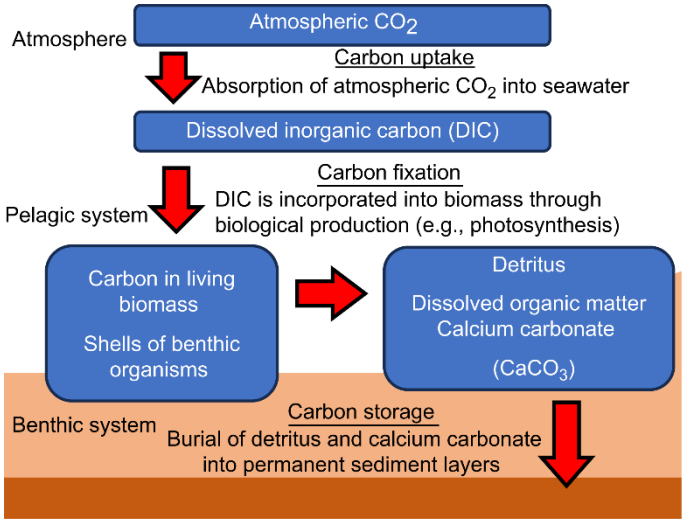

https://doi.org/10.5194/egusphere-2026-2710
Preprint. Discussion started: 4 June 2026

Figure 1. Conceptual diagram of climate-change mitigation functions in coastal ecosystems. Atmospheric CO_2 is absorbed into seawater through air–sea CO_2 exchange (carbon uptake). Dissolved inorganic carbon (DIC) is subsequently incorporated into biological biomass through photosynthesis and shell formation (carbon fixation). Part of the fixed carbon is transported to the benthic system as detritus, dissolved organic matter, and calcium carbonate, and is eventually buried in deeper sediment layers (carbon storage).

2 Model overview and characteristics

Existing process-based marine ecosystem models have been developed to represent lower-trophic biogeochemistry and benthic–pelagic water–sediment coupling in coastal and marine systems (Butenschön et al., 2016; Yakushev et al., 2017). EMAGIN-B.C. (Sohma et al., 2018) is a coupled ecosystem model that integrates climate-change mitigation functions in coastal shallow waters through a sequence of carbon cycling processes. These processes include air–sea CO_2 flux, biological fixation of CO_2 into organic matter and calcium carbonate through biological production, and burial and sequestration of carbon in deeper sediment layers.

This model explicitly couples pelagic–benthic interactions, carbonate chemical equilibrium, sediment remineralization processes, $CaCO_3$ formation, and changes in biological production structure within a unified modelling framework. Therefore, the model enables analysis of how variations in nutrient loading influence carbon uptake, fixation, and storage functions in three contrasting coastal regions—estuarine, central bay, and tidal-flat environments—not merely as quantitative changes but as shifts in the relative dominance of the processes governing carbon cycling.

2.1 Model structure

2.1.1 Carbonate chemical equilibrium

The model calculates the production and consumption of DIC and TA associated with biological and chemical processes. At each time step, the carbonate equilibrium system of DIC–TA–pH–pCO_2 is solved. The individual carbonate species of DIC (H_2CO_3, HCO_3^-, and CO_3^{2-}) are determined using equilibrium relationships. Through this structure, variations in DIC and TA induced by biological and chemical processes are reflected in air–sea CO_2 fluxes via changes in pCO_2.

2.1.2 Microbial remineralization processes

Organic matter remineralization is divided into three pathways: aerobic, suboxic, and anaerobic. The model calculates the production and consumption of DO, NH_4–N, NO_3–N, PO_4–P, DIC, and TA associated with remineralization, nitrification, and oxidation of oxygen demand units (reduced compounds such as Mn^{2+}, Fe^{2+}, and sulphide). These processes are explicitly

https://doi.org/10.5194/egusphere-2026-2710
Preprint. Discussion started: 4 June 2026

coupled with the carbonate chemical equilibrium system within the integrated framework shown in **Fig. 2**, thereby influencing air–sea CO_2 fluxes.

2.1.3 Physiological–ecological and food-web structure

The nutrient–phytoplankton–zooplankton–detritus (NPZD) framework is extended to include the benthic system. The food web linking phytoplankton, benthic algae, zooplankton, benthic fauna, and detritus is explicitly represented. Carbon transport from primary production to higher trophic levels through grazing enables evaluation of the carbon fixation function. $CaCO_3$ formation by suspension feeders is also explicitly incorporated.

2.1.4 Three-pool organic matter structure

Organic matter is represented as three fractions: labile, semi-labile, and refractory pools. The remineralization rate decreases progressively among these fractions. This structure allows the model to distinguish between short-term remineralization fluxes and long-term burial fluxes. Refractory organic matter is transferred to permanent sediment layers, thereby strengthening the carbon storage function, whereas labile organic matter is remineralized and returned to the pelagic system.

2.1.5 Coupled cycles of carbon, nitrogen, phosphorus, and oxygen

The carbon cycle is governed by nutrient concentrations and dissolved oxygen (DO) conditions. Nutrients control photosynthetic production, whereas hypoxic conditions alter mortality and metabolic activity of benthic organisms. By simultaneously solving the coupled carbon, nitrogen, phosphorus, and oxygen (C–N–P–O) cycles, the model dynamically links carbonate chemistry, remineralization processes, and food-web dynamics within a unified biogeochemical framework.

2.1.6 Pelagic–benthic coupling

Pelagic and benthic systems are explicitly coupled through sedimentation, resuspension, and material exchange, thereby linking carbon uptake, fixation, and storage processes within a consistent framework.

2.1.7 Coupling with physical transport

Advection and diffusion across offshore boundaries are explicitly considered in calculating carbon inflow and outflow, thereby linking physical transport processes to regional variability in model responses.

2.2 Model improvements (ver. 2)

In this study, the original EMAGIN-B.C. model of Sohma et al. (2018) is extended with the following improvements.

https://doi.org/10.5194/egusphere-2026-2710
Preprint. Discussion started: 4 June 2026

(a) Physiological and metabolic responses dependent on pH are introduced to incorporate the effects of ocean acidification (Omachi and Sohma, 2022, 2023).

(b) The remineralization rate formulation is extended based on microbial ATP production efficiency dependent on oxygen conditions (Ishizuka and Sohma, 2025).

This modification enables the model to dynamically adjust remineralization rates according to oxygen conditions, resulting in reduced decomposition under hypoxic conditions and enhanced differentiation of remineralization processes across redox environments compared with those of ver. 1.

The improved version used in this study is referred to as EMAGIN-B.C. ver. 2. **Figs 2(a) and (b)** show the detailed biological and chemical process structures of the pelagic and benthic systems, respectively. **Table 1** lists the corresponding state variables of the model. **Fig. 3** conceptually illustrates the coupled structure of the DIC and TA production–consumption processes, physical transport, carbonate equilibrium, and the state-variable updating algorithm at each time step.

https://doi.org/10.5194/egusphere-2026-2710
Preprint. Discussion started: 4 June 2026

(a) Pelagic system

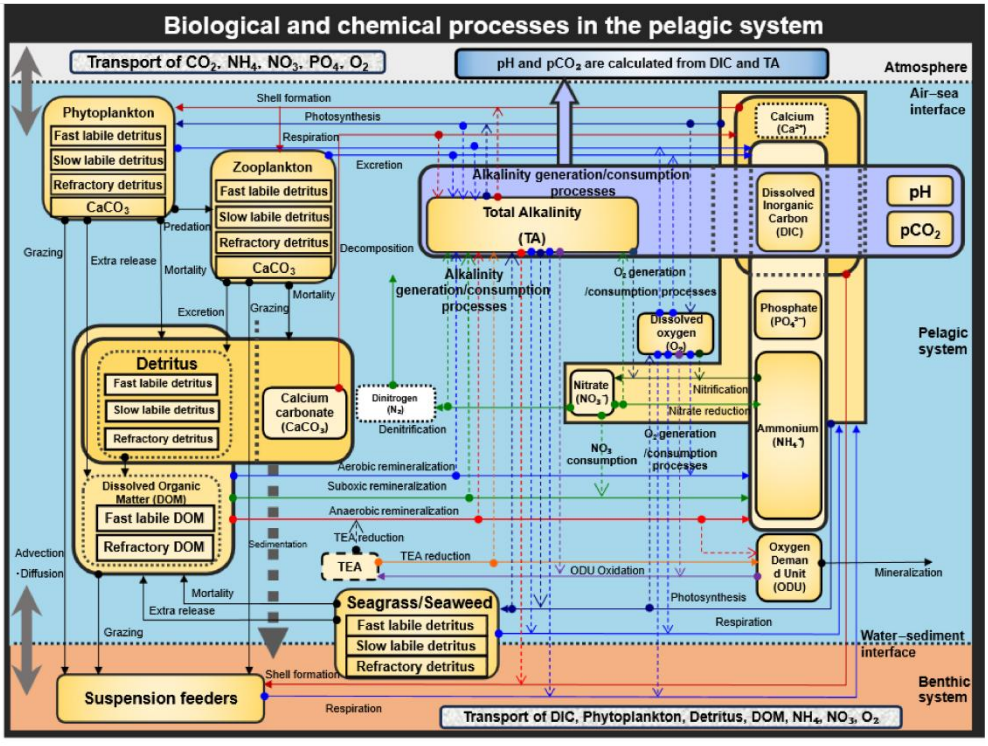

(b) Benthic system

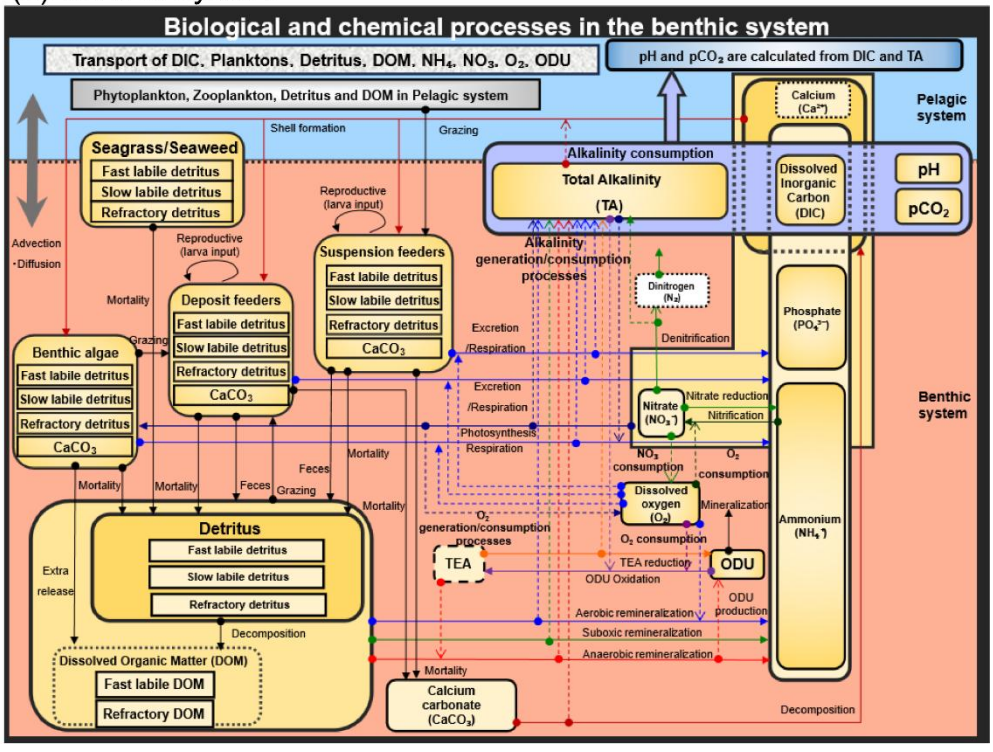

https://doi.org/10.5194/egusphere-2026-2710
Preprint. Discussion started: 4 June 2026

Figure 2. Ecosystem structure of the EMAGIN-B.C. coupled ecosystem model: (a) pelagic system; (b) benthic system. Boxes represent model state variables, and arrows indicate biological and chemical processes including material fluxes linking biological production, microbial remineralization, and carbonate chemistry.

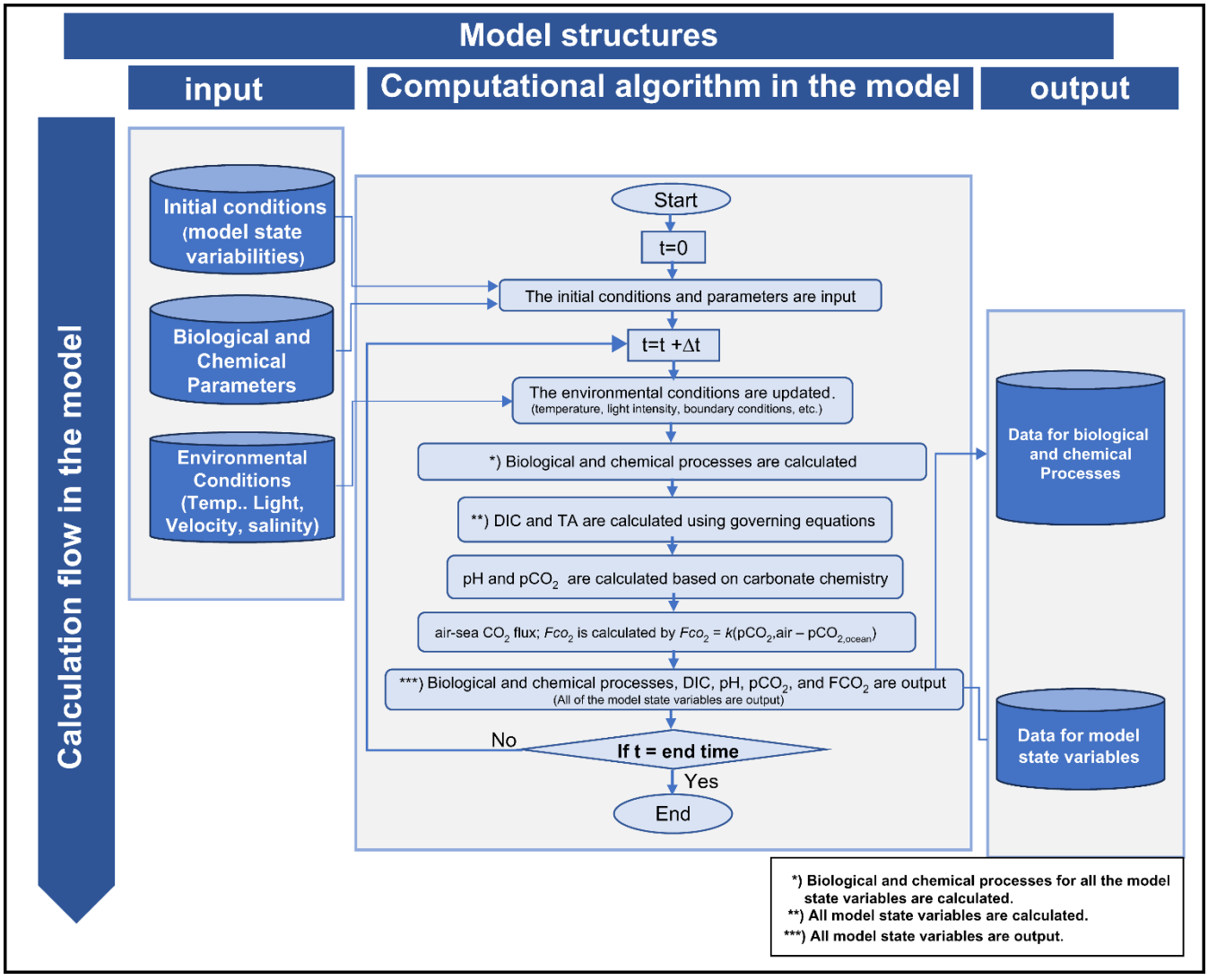

Figure 3. Conceptual diagram of the coupled structure among DIC and TA production–consumption processes, physical transport, carbonate chemical equilibrium, and the state-variable updating algorithm at each time step. DIC, dissolved inorganic carbon; TA, total alkalinity; pCO_2, partial pressure of CO_2; FCO_2, air–sea CO_2 flux.

https://doi.org/10.5194/egusphere-2026-2710
Preprint. Discussion started: 4 June 2026

Table 1. Model state variables in EMAGIN-B.C.

System	State variable	Unit	Symbol in diagram
Pelagic system	Phytoplankton	mgC L^{-1}	Phytoplankton
Pelagic system	Zooplankton	mgC L^{-1}	Zooplankton
Pelagic system	Fast labile detritus	mgC L^{-1}	Fast labile detritus
Pelagic system	Slow labile detritus	mgC L^{-1}	Slow labile detritus
Pelagic system	Refractory detritus	mgC L^{-1}	Refractory detritus
Pelagic system	Labile dissolved organic matter	mgC L^{-1}	Labile DOM
Pelagic system	Refractory dissolved organic matter	mgC L^{-1}	Refractory DOM
Pelagic system	Ammonium nitrogen	mgN L^{-1}	NH_4
Pelagic system	Nitrate nitrogen	mgN L^{-1}	NO_3
Pelagic system	Phosphate phosphorus	mgP L^{-1}	PO_4
Pelagic system	Reduced substances	mg L^{-1}	ODU
Pelagic system	Dissolved oxygen	mgO_2 L^{-1}	O_2
Pelagic system	Dissolved inorganic carbon	mgC L^{-1}	DIC
Pelagic system	Calcium	mgCa L^{-1}	Ca
Pelagic system	Calcium carbonate	mgC L^{-1}	$CaCO_3$
Pelagic system	Total alkalinity	meq L^{-1}	TALK
Pelagic system	Partial pressure of CO_2	µatm	pCO_2
Pelagic system	pH	–	pH
Benthic system	Suspension feeders	µgC cm^{-2} sediment	Suspension feeders
Benthic system	Deposit feeders	µgC cm^{-2} sediment	Deposit feeders
Benthic system	Benthic algae	µgC cm^{-2} sediment	Benthic algae
Benthic system	Fast labile detritus	µgC cm^{-3} sediment solid	Fast labile detritus
Benthic system	Slow labile detritus	µgC cm^{-3} sediment solid	Slow labile detritus
Benthic system	Refractory detritus	µgC cm^{-3} sediment solid	Refractory detritus

https://doi.org/10.5194/egusphere-2026-2710
Preprint. Discussion started: 4 June 2026

Benthic system	Labile dissolved organic matter	mgC L^{-1}	Labile DOM
Benthic system	Refractory dissolved organic matter	mgC L^{-1}	Refractory DOM
Benthic system	Ammonium nitrogen	mgN L^{-1}	NH_4
Benthic system	Nitrate nitrogen	mgN L^{-1}	NO_3
Benthic system	Phosphate phosphorus	mgP L^{-1}	PO_4
Benthic system	Reduced substances	mg L^{-1}	ODU
Benthic system	Dissolved oxygen	mg O_2 L^{-1}	O_2
Benthic system	Calcium carbonate	µgC cm^{-2} sediment	$CaCO_3$

Note**:** Pelagic variables are expressed per unit water volume (mg L^{-1} or mgC L^{-1}). Benthic biomass is expressed per unit sediment surface area (µgC cm^{-2}), whereas sediment detritus is expressed per unit sediment solid volume (µgC cm^{-3}). Functional groups such as bivalves (suspension feeders) and polychaetes (deposit feeders) represent the dominant benthic taxa in Tokyo Bay.

3 Model application and simulation setup

In this study, Tokyo Bay was selected as the target coastal system, because it represents a semi-enclosed inner bay characterised by strong spatial heterogeneity in both physical and biogeochemical environments. The EMAGIN-B.C. ver. 2 model was applied to this system. Tokyo Bay exhibits large gradients in water depth, nutrient loading, and water exchange characteristics from the river mouth to the central bay and tidal-flat regions. These features make the bay a representative system for examining how variations in external loading influence carbon cycling processes in heterogeneous coastal environments.

Fig. 4 shows the computational domain and grid configuration. The horizontal domain is divided into 26 boxes, forming a box-model framework that reflects the bathymetry and geomorphological characteristics of the bay. In the vertical direction, the pelagic system is discretised at 2-m intervals. In the benthic system, the upper 10 cm of sediment is divided into 30 layers. The sediment layer thickness is set to be finer near the sediment surface and gradually increases with depth, ranging from 0.1 mm to 1.2 cm. This configuration allows the model to resolve steep oxygen gradients and the associated aerobic, suboxic, and anaerobic mineralization processes occurring within the surface sediment with high resolution.

The model includes 33 state variables representing pelagic and benthic components (**Table 1**). External forcing conditions include freshwater inflow, nutrient loading, solar radiation, wind stress, and open boundary conditions at the mouth of the bay. These forcings are prescribed as annual periodic functions based on observational data from 1998–2002. This period represents a pre-intensive nutrient management phase characterised by typical seasonal variability and recurrent hypoxic conditions and is therefore suitable as a baseline for evaluating system responses to changes in nutrient loading.

https://doi.org/10.5194/egusphere-2026-2710
Preprint. Discussion started: 4 June 2026

Long-term simulations are conducted under these periodic forcings until the system reaches a periodic steady state in which state variables reproduce a stable annual cycle. This periodic steady state is not intended to reproduce a specific year but to represent a dynamically equilibrated seasonal cycle under the given forcing conditions.

This state is interpreted as representing the typical seasonal ecosystem conditions of Tokyo Bay around the year 2000. Subsequent analyses compare this baseline state with various nutrient loading scenarios described in the following sections.

Detailed model settings for the control case follow those described in Sohma et al. (2018). The response of carbon cycling to variations in external loading was examined using this model configuration.

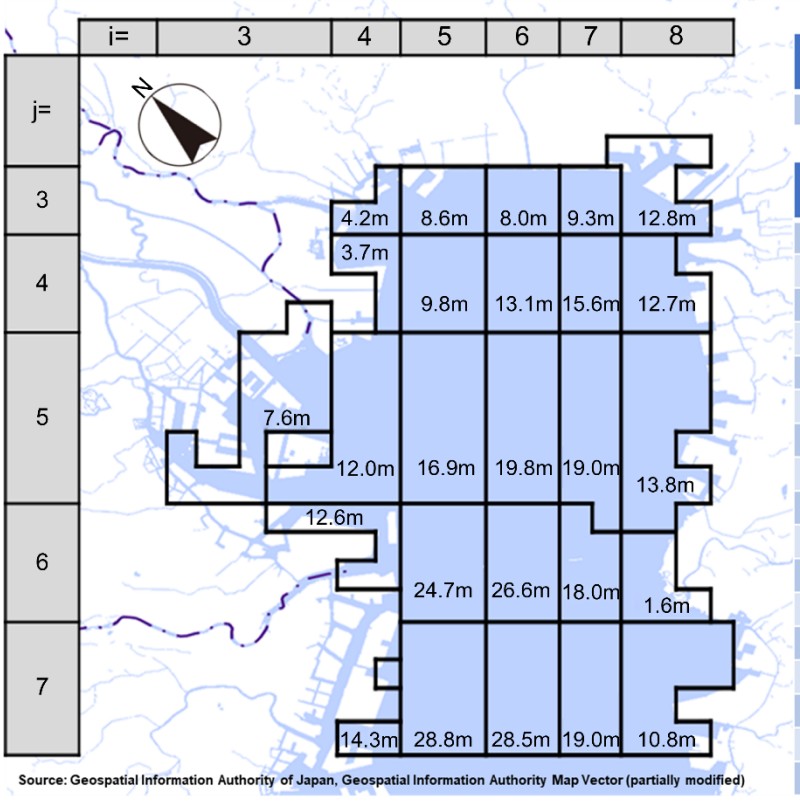

Pelagic system

Depth [m]	Thickness of layer [m]
0-Bottom	2.0

Benthic system

Depth [cm]	Thickness of layer [cm]
0-0.05	0.01
0.05-0.08	0.015
0.08-0.1	0.02
0.1-0.16	0.03
0.16-0.2	0.04
0.2-0.3	0.05
0.3-0.42	0.06
0.42-0.5	0.08
0.5-0.6	0.1
0.6-0.9	0.15
0.9-1.1	0.2
1.1-1.4	0.3
1.4-1.8	0.4
1.8-2.4	0.6
2.4-3.2	0.8
3.2-5.2	1.0
5.2-10	1.2

Figure 4. Computational domain and grid configuration of the EMAGIN-B.C. model for Tokyo Bay. The bay is represented by 26 horizontal boxes reflecting the bathymetry of the bay. The pelagic system is vertically discretised at 2-m intervals, while the upper 10 cm of sediment in the benthic system is divided into 30 layers with finer resolution near the sediment surface.

https://doi.org/10.5194/egusphere-2026-2710
Preprint. Discussion started: 4 June 2026

4 Model validation

Model performance was evaluated through comparison of simulated results with observational data for state variables including phytoplankton biomass (PP), particulate organic carbon (POC), DO, nitrate nitrogen (NO_3), ammonium nitrogen (NH_4), phosphate phosphorus (PO_4), dissolved organic carbon (DOC), and total organic carbon (TOC).

As shown in **Table 2**, DO and major inorganic nutrients (NO_3 and PO_4) exhibit moderate-to-high correlations (R = 0.6–0.8). Bottom-layer DO exhibits a high correlation (R = 0.82), indicating good model performance. It also reflects the integrated outcome of organic matter decomposition and mineralization processes. Therefore, its high reproducibility suggests that the model appropriately represents the dynamical coupling among key processes such as primary production, particle sinking, organic matter decomposition, and vertical mixing.

In contrast, the correlations for PP and POC in the bottom layer are relatively low, indicating limitations in reproducing localised biological processes and short-term resuspension events. This study does not aim to reproduce short-term variability but to evaluate the relative dominance of governing processes under varying external loading conditions. In this context, the satisfactory reproduction of process-integrated indicators such as DO and inorganic nutrients supports the validity of the mechanistic analyses conducted in this study. The model represents interactions among multiple state variables in an integrated manner, with a reasonable level of reproducibility confirmed for several key variables.

Although the model tends to underestimate bottom-layer PP and POC, these discrepancies are primarily attributed to limitations in observational data and localised benthic–pelagic interactions. Therefore, the dominant relationships among processes are largely preserved across regions, and these discrepancies do not substantially affect the interpretation of spatial differentiation in carbon-control structures, including relative changes in benthic carbon storage, as shown in **Figs. 5(A) and (B).**

At the representative grid cells shown in **Figs. 5(A) and (B)**, the model generally reproduces seasonal patterns in both surface and bottom layers. In particular, the model successfully captures the development of bottom hypoxia during summer and its recovery during winter.

Overall, the model reproduces the seasonal-scale structure of carbon cycling and nutrient dynamics in Tokyo Bay and is therefore suitable for analysing mechanistic responses to variations in external loading.

https://doi.org/10.5194/egusphere-2026-2710
Preprint. Discussion started: 4 June 2026

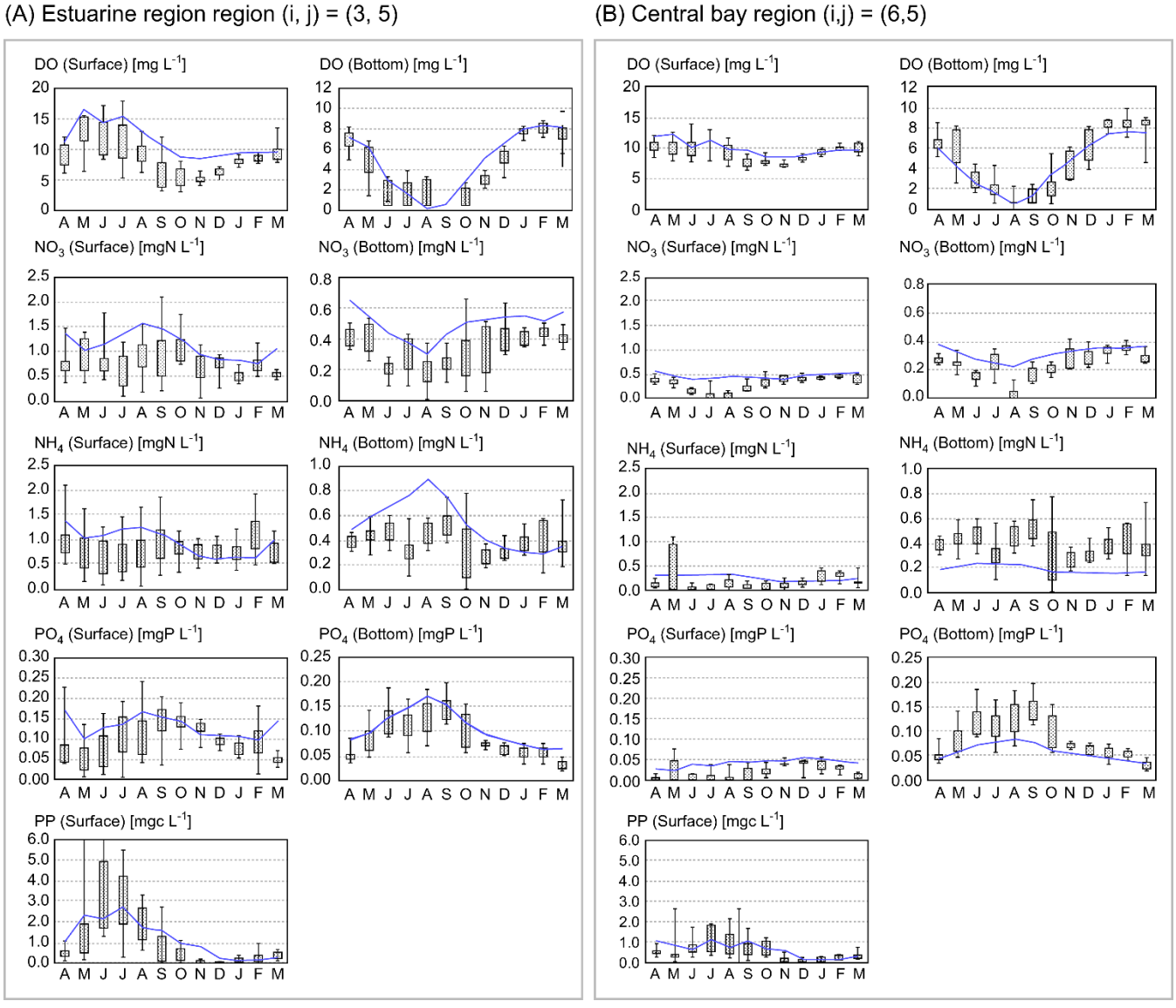

Figure 5. Comparison between simulated and observed seasonal variations of state variables at representative grid cells in Tokyo Bay: (A) estuarine region (i, j) = (3, 5) and (B) central bay (i, j) = (6, 5). The blue line indicates model results, and box plots represent monthly observational data. Boxes show the first and third quartiles, and whiskers indicate the minimum and maximum values. Surface and bottom denote the upper and lower layers of the water column, respectively. PP, phytoplankton biomass; POC, particulate organic carbon; DOC, dissolved organic carbon; DO, dissolved oxygen; NO_3, nitrate nitrogen; NH_4, ammonium nitrogen; PO_4, phosphate phosphorus.

https://doi.org/10.5194/egusphere-2026-2710
Preprint. Discussion started: 4 June 2026

Table 2. Statistical comparison between model results and observations for the EMAGIN-B.C. model. Evaluation metrics include correlation coefficient (R), root mean square error (RMSE), mean observed value, p-value, and number of observations (N).

Variable	Layer	R	RMSE	Mean observation	p-value	N
DO	Surface	0.43	2.19	8.85	<0.01	232
	Bottom	0.82	1.68	5.43	<0.01	232
NO_3	Surface	0.71	0.21	0.41	<0.01	232
	Bottom	0.61	0.13	0.27	<0.01	232
NH_4	Surface	0.59	0.25	0.34	<0.01	232
	Bottom	0.39	0.15	0.20	<0.01	232
PO_4	Surface	0.64	0.03	0.05	<0.01	232
	Bottom	0.46	0.03	0.05	<0.01	232
PP	Surface	0.41	0.94	0.76	<0.01	232
	Bottom	0.14	0.18	0.17	0.16	100
POC	Surface	0.31	0.27	0.30	<0.01	100
	Bottom	0.24	0.24	0.18	0.04	76
DOC	Surface	0.41	1.03	2.13	<0.01	100
	Bottom	0.47	0.35	1.43	<0.01	70
TOC	Surface	0.80	0.83	2.99	<0.01	100
	Bottom	0.55	0.49	1.85	<0.01	78

Note: R: correlation coefficient between model results and observations; RMSE: root mean square error; mean observation: average of observed values; N: number of observations. DO: dissolved oxygen (mg L^{-1}); NO_3: nitrate nitrogen (mgN L^{-1}); NH_4: ammonium nitrogen (mgN L^{-1}); PO_4: phosphate phosphorus (mgP L^{-1}); PP: phytoplankton biomass (mgC L^{-1}); POC: particulate organic carbon (mgC L^{-1}); DOC: dissolved organic carbon (mgC L^{-1}); TOC: total organic carbon (mgC L^{-1}). Surface and bottom indicate the upper and lower layers of the water column, respectively.

5 Scenario design and evaluation framework for ecosystem carbon functions

In this study, we examine how variations in riverine loads of dissolved inorganic nitrogen (DIN) and dissolved inorganic phosphorus (DIP) influence three climate-mitigation functions of the coastal ecosystem in Tokyo Bay—carbon uptake, carbon fixation, and carbon storage. This section describes the loading scenarios, evaluation indicators, and analysis regions used in the sensitivity analyses.

https://doi.org/10.5194/egusphere-2026-2710
Preprint. Discussion started: 4 June 2026

5.1 Riverine loading scenarios

Riverine inputs of DIN and DIP to Tokyo Bay are the primary control variables in the sensitivity analysis. DIN is defined as the sum of NH_4^+ and NO_3^-, while DIP is represented by PO_4^{3-}.

Relative to the baseline control case, four loading scenarios were defined by simultaneously changing DIN and DIP loads to 0.5, 2.0, 3.0, and 5.0 times the control level. These multipliers represent a wide range of plausible variations in nutrient loading, encompassing both reduced conditions and potential increases under intensified anthropogenic influences. This design allows evaluation of the system response to changes in total nutrient load while maintaining a constant N:P ratio in the inflowing river water.

DIN and DIP loads were introduced into the surface layer (Layer 1) of fourteen computational boxes (①–⑭) shown in **Fig. 6**. In contrast, freshwater inflow, meteorological conditions, and open-boundary conditions were kept identical across all scenarios and were prescribed using periodic forcing functions derived from observational data for 1998–2002, as described in **Sect. 3**. Thus, DIN and DIP loading is treated as the only independent variables in the sensitivity experiments.

Each scenario simulation was performed for sufficiently long periods under periodic forcing until all state variables reached a stable annual cycle. The resulting periodic equilibrium state for each loading scenario was used for analysis. Structural responses to loading changes are evaluated by comparing these equilibrium states with the control case to identify changes in the dominant processes governing carbon cycling.

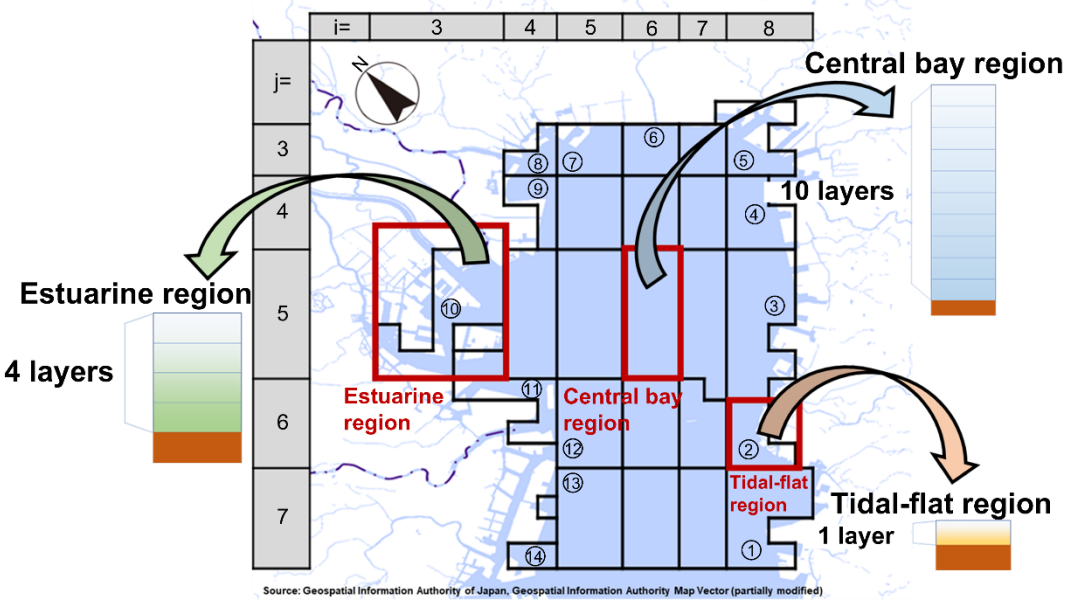

Figure 6. Spatial distribution of riverine nutrient loading points (①–⑭) in the EMAGIN-B.C. computational domain and the three representative regions analysed in this study: estuarine region ((i, j) = (3, 5)), central bay region ((i, j) = (6, 5)), and tidal-flat region ((i, j) = (8, 6)). Numbers (①–⑭) indicate grid cells where riverine nutrient loads are introduced into the surface layer of

https://doi.org/10.5194/egusphere-2026-2710
Preprint. Discussion started: 4 June 2026

the model. These regions represent contrasting ecological environments within Tokyo Bay, characterised by differences in nutrient loading, water depth, and benthic–pelagic coupling. Schematic diagrams illustrate the vertical structures used in the model for each region.

5.2 Evaluation indicators

Based on the conceptual framework described in **Sects. 1 and 2**, three ecosystem carbon-cycle functions are defined and quantified using the following operational definitions.

5.2.1 Carbon uptake function: air–sea CO_2 flux

The carbon uptake function is defined based on the air–sea CO_2 exchange flux in the surface layer of the pelagic system:

$$F_{CO_2} = k\left(pCO_{2,air} - pCO_{2,ocean}\right) \quad (1)$$

where k is the gas transfer coefficient, calculated based on wind speed following the parameterization of Wanninkhof (2014), and $pCO_{2,\mathrm{ocean}}$ is the partial pressure of CO_2 in seawater calculated within the model from the carbonate equilibrium system (DIC–TA–pH–pCO_2) (see **Fig. 2**). In this study, flux from the atmosphere to the ocean is defined as positive.
This flux reflects the integrated effects of multiple processes, including biological production, remineralization, carbonate formation, and physical mixing and therefore serves as an integrated indicator of the ecosystem metabolic state. Owing to its strong short-term variability, both the time series of 10-day moving averages and annual mean values are evaluated to assess temporal variations and long-term changes in carbon uptake.

5.2.2 Carbon fixation function: biological capture of DIC

The carbon fixation function is defined as the net biological consumption of DIC, including photosynthesis by phytoplankton and benthic algae as well as $CaCO_3$ formation associated with suspension feeders.
The temporal change in DIC is governed by the combined effects of the following biological and chemical processes:

- DIC consumption by photosynthesis;
- DIC production by respiration and remineralization;
- DIC consumption by $CaCO_3$ formation;
- DIC production by $CaCO_3$ dissolution.

The DIC budget integrated over the entire pelagic water column is calculated using annual mean values and 10-day moving averages. Net DIC consumption represents the carbon capture capacity of biological production and carbonate formation processes and therefore serves as the operational indicator of the carbon fixation function.

https://doi.org/10.5194/egusphere-2026-2710
Preprint. Discussion started: 4 June 2026

5.2.3 Carbon storage function: burial flux of organic matter and $CaCO_3$

The carbon storage function is defined based on the burial flux of organic matter and $CaCO_3$ that becomes permanently sequestered in deeper sediment layers.

The burial of sedimentary organic matter is regulated by competition with remineralization processes, the rates of which depend strongly on sediment oxygen conditions (aerobic, suboxic, and anoxic environments). Burial is also influenced by benthic faunal feeding, population density, and mortality associated with hypoxia. Therefore, the storage function emerges as the result of dynamical interactions among biological and biogeochemical processes, rather than simply reflecting the sedimentation flux.

Both annual mean values and 10-day moving averages were evaluated to assess temporal variability and long-term changes in the carbon storage function.

5.3 Analytical framework for relative responses of carbon-cycle functions

In addition to evaluating absolute changes in each function, this study focuses on differences in response magnitude and seasonal phase shifts among the three functions under varying nutrient loading conditions. Although carbon uptake, fixation, and storage are mutually coupled processes, each function is governed by different dominant mechanisms and, therefore, does not necessarily respond in the same manner to nutrient loading.

Accordingly, annual mean values and seasonal variability patterns are compared among scenarios to identify which function exhibits the strongest response to loading changes. This approach enables mechanistic interpretation of shifts in the dominant processes governing carbon cycling.

5.4 Analysis regions: estuarine region, central bay region, and tidal-flat region

Because ecosystem responses to nutrient loading depend strongly on regional environmental characteristics, analyses are conducted for three representative regions with contrasting ecological properties, as shown in **Fig. 6**:

- Estuarine region ((i, j) = (3, 5)): strongly influenced by major river inputs, characterised by high nutrient concentrations and high suspended matter, where primary production responses are pronounced (mean depth: 7.6 m).
- Central bay region ((i, j) = (6, 5)): representative of the broader Tokyo Bay environment and important for evaluating basin-scale material budgets (mean depth: 19.8 m).
- Tidal-flat region ((i, j) = (8, 6)): shallow and well-illuminated environments, where benthic algae and benthic fauna contribute strongly and benthic–pelagic coupling is particularly strong (mean depth: 1.6 m).

The EMAGIN-B.C. model enables comparative evaluation of carbon uptake, fixation, and storage functions across these regions within a unified modelling framework.

https://doi.org/10.5194/egusphere-2026-2710
Preprint. Discussion started: 4 June 2026

6 Mechanistic hypotheses for carbon uptake, fixation, and storage (theoretical framework)

Based on the scenario analysis, the carbon-cycle structure inherent in EMAGIN-B.C. ver. 2 is interpreted as a dual-loop system consisting of organic and carbonate pathways. Within this framework, the major mechanisms emerging in response to nutrient loading are systematically organised.

EMAGIN-B.C. ver. 2 has a structure that represents (i) the organic-matter supply flux mediated by photosynthesis, food-web transfer, and sedimentation, (ii) the calcium carbonate formation flux governed by shell production, (iii) the remineralization flux based on microbial mineralization, and (iv) the calcium carbonate dissolution flux that proceeds under low-pH conditions. These four fluxes are dynamically redistributed through mutual coupling via the carbonate equilibrium system (DIC–TA–pH–pCO_2).

Accordingly, carbon uptake, carbon fixation, and carbon storage are interpreted as dynamic imbalances between supply-side fluxes (organic-matter supply and $CaCO_3$ formation) and loss-side fluxes (remineralization and $CaCO_3$ dissolution). Importantly, the dominant roles of these fluxes vary depending on the temporal scale. Carbon uptake emerges as a short-term response (from several days to seasonal scales) through the immediate redistribution of the carbonate equilibrium system. Carbon fixation responds on seasonal to annual scales through changes in biomass carbon and solid-phase inorganic carbon. Carbon storage, in contrast, emerges as a long-term response over annual to decadal timescales, because it is determined by the competition among sedimentation, remineralization, dissolution, and burial processes.

Based on this hierarchical temporal structure, this section organises the dominant mechanisms operating at short-term (**Sect. 6.1**), medium-term (**Sect. 6.2**), and long-term (**Sect. 6.3**) timescales and provides a mechanistic basis for interpreting the scenario-analysis results presented in **Sect. 7**.

6.1 Mechanistic hypotheses for carbon uptake and release

Carbon uptake (air–sea CO_2 flux) is **the most rapidly responding carbon-mitigation function** among the three functions. This response emerges on timescales ranging from several days to seasonal scales through the redistribution of the carbonate equilibrium system (DIC–TA–pH–pCO_2).

In EMAGIN-B.C. ver. 2, short-term responses are primarily controlled by (a) immediate changes in photosynthetic production and remineralization fluxes within the organic carbon pathway and (b) changes in TA associated with $CaCO_3$ formation and dissolution within the carbonate pathway. These fluxes are coupled through the carbonate equilibrium system and can rapidly shift the air–sea CO_2 flux toward either uptake or release.

Accordingly, the principal pathways that emerge in response to nutrient enrichment are classified into uptake mechanisms (A1–A3) and release mechanisms (R1–R3) (**Fig. 7**).

https://doi.org/10.5194/egusphere-2026-2710
Preprint. Discussion started: 4 June 2026

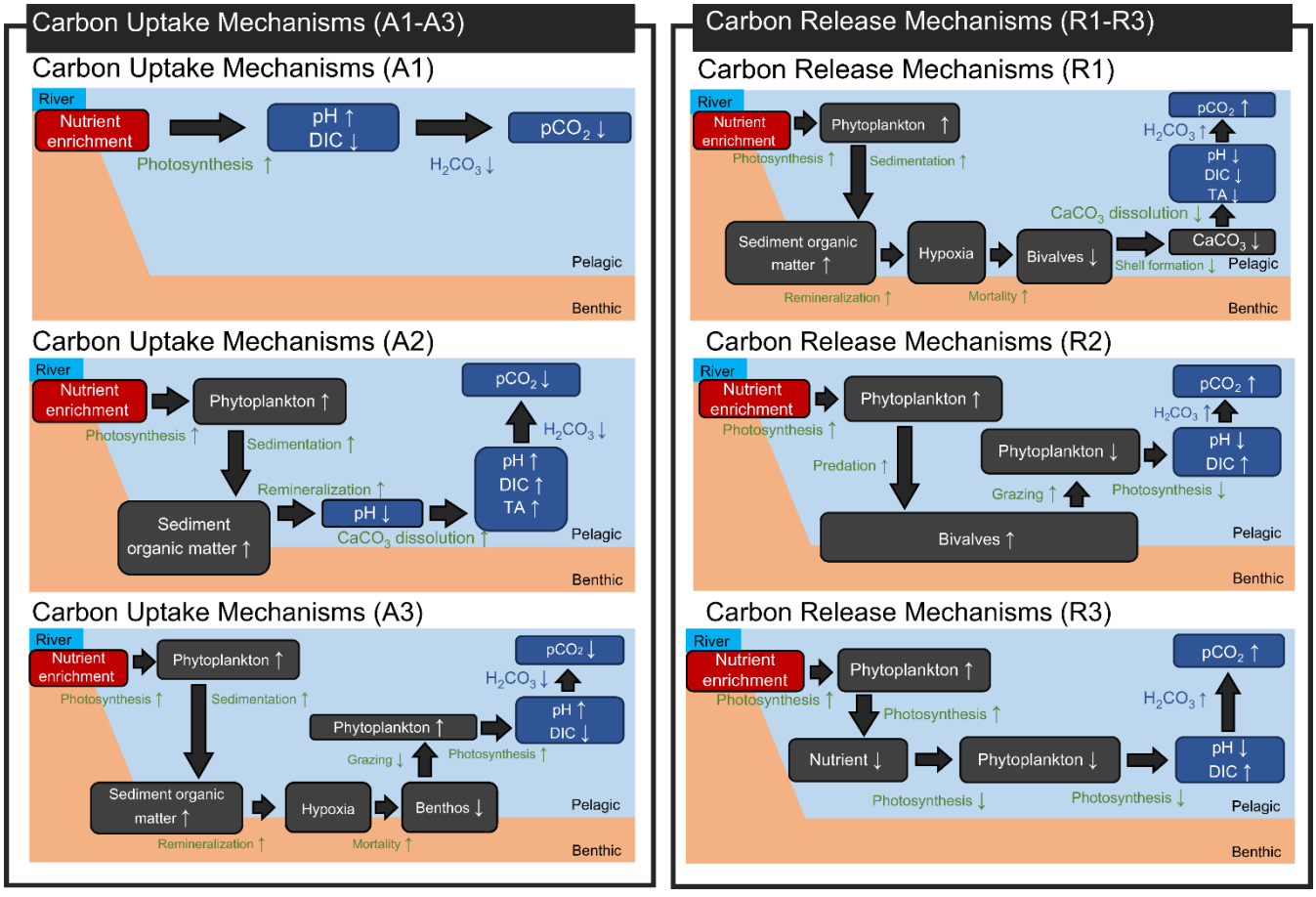

Figure 7. Conceptual diagram of three carbon uptake mechanisms (A1–A3) and three carbon release mechanisms (R1–R3) that emerge in EMAGIN-B.C. ver. 2 under increasing nutrient loading. Each panel illustrates a causal pathway linking (i) environmental forcing (nutrient enrichment), (ii) biological and biogeochemical processes (e.g., photosynthesis, organic-matter sedimentation, hypoxia development, shell formation and dissolution, and changes in grazing pressure), and (iii) responses of the carbonate system (DIC, TA, pH, and pCO_2). These interacting processes ultimately drive shifts in the air–sea CO_2 flux toward either atmospheric CO_2 uptake (A1–A3) or release (R1–R3). Arrows indicate causal relationships originating from nutrient enrichment shown on the left side of each panel. Blue frames represent pelagic processes, whereas orange frames represent benthic processes. Color-coded boxes indicate environmental forcing (red), biological and biogeochemical processes (green), and carbonate-system responses (blue). Upward (↑) and downward (↓) arrows denote increases and decreases in the corresponding variables or fluxes, respectively.

6.1.1 Uptake mechanisms (A-mechanisms)

(1) A1: Pelagic photosynthetic DIC drawdown

https://doi.org/10.5194/egusphere-2026-2710
Preprint. Discussion started: 4 June 2026

An increase in nutrient concentration enhances phytoplankton photosynthesis and increases the organic-matter supply flux. As a result, DIC decreases, pH increases, and pCO_2 declines. This shift drives the air–sea CO_2 flux toward the uptake direction. This mechanism **constitutes a short-term uptake pathway** driven by an increase in the supply flux within the organic carbon pathway and is completed entirely within the pelagic system.

Short-term implication: *During production-dominated periods, the net CO_2 flux shifts toward atmospheric uptake.*

(2) A2: Benthic remineralization-induced $CaCO_3$ dissolution

Enhanced primary production resulting from nutrient enrichment increases the supply flux of settling organic matter to the sediments. When remineralization intensifies within the sediments, pH decreases in bottom and pore waters, promoting $CaCO_3$ dissolution. In the model, $CaCO_3$ dissolution is parameterised as a function of the calcite saturation state (Ω), following Sohma et al. (2018), while recognising that in shallow coastal environments, dissolution processes are also influenced by biological activity and sediment microenvironments.

$CaCO_3$ dissolution increases TA, thereby redistributing the carbonate equilibrium system and lowering pCO_2. When this low-pCO_2 water mass is transported to the surface through vertical mixing, the air–sea CO_2 flux shifts toward atmospheric uptake. This mechanism constitutes an indirect uptake pathway, in which increased remineralization within the organic carbon pathway induces dissolution fluxes within the carbonate pathway through dual-loop coupling.

Short-term implication: *When benthic remineralization is dominant and vertical mixing occurs, CO_2 uptake is secondarily enhanced.*

(3) A3: Hypoxia-induced predator release

Excess nutrient supply increases the flux of settling organic matter and enhances remineralization, thereby promoting hypoxia in the bottom waters. Mild-to-moderate hypoxia reduces the biomass of benthic organisms and weakens the grazing pressure on phytoplankton. The reduction in grazing pressure increases PP and amplifies the organic matter supply flux through enhanced photosynthesis, thereby increasing CO_2 uptake. This mechanism constitutes a short-term uptake pathway driven by the food-web structure within the organic carbon pathway. However, if hypoxia intensifies further, ecosystem collapse may occur, and the system may shift to the supply-reduction pathway described in D1.

Short-term implication: *Mild-to-moderate hypoxia can enhance CO_2 uptake in the short term, whereas severe hypoxia may eventually weaken uptake.*

6.1.2 Release mechanisms (R-mechanisms)

(1) R1: Loss of benthic calcifiers (decline in shell formation)

https://doi.org/10.5194/egusphere-2026-2710
Preprint. Discussion started: 4 June 2026

When hypoxia progresses, the biomass of calcifying organisms decreases, and $CaCO_3$ formation flux declines. A reduction in $CaCO_3$ formation decreases TA, which raises pCO_2 through the carbonate equilibrium system. As a result, the air–sea CO_2 flux shifts toward atmospheric release. This mechanism constitutes a short-term release pathway driven by a reduction in formation flux within the carbonate pathway.

Notably, although both R1 and A3 originate from hypoxia, they represent branching responses: A3 amplifies organic-carbon supply, whereas R1 promotes CO_2 release through carbonate-system effects.

Short-term implication: *If calcifying organisms decline substantially, the CO_2 flux shifts toward net release.*

(2) R2: Seasonal grazing surge (suppression of photosynthesis by suspension feeders)

Nutrient enrichment increases phytoplankton and zooplankton abundance, which improves the food environment for suspension feeders and increases their biomass. Stronger grazing pressure suppresses phytoplankton photosynthesis and reduces the organic-matter supply flux. As a result, DIC increases, pH decreases, and pCO_2 rises through the carbonate equilibrium system, shifting the air–sea CO_2 flux toward atmospheric release. This mechanism constitutes a short-term release pathway driven by suppression of the supply flux within the organic carbon pathway and corresponds to a response symmetric to the supply-amplification pathway described in A1.

Short-term implication: *During seasons when grazing pressure dominates, peaks in CO_2 release emerge.*

(3) R3: Post-bloom DIC accumulation

Nutrient enrichment can trigger phytoplankton blooms, which subsequently collapse when nutrients become depleted. After bloom collapse, the organic-matter supply flux declines while remineralization becomes dominant. As a result, DIC increases again and pCO_2 rises through the carbonate equilibrium system. This mechanism **constitutes a decomposition-dominated release pathway** within the organic carbon pathway and generates a phase-lagged response between production-dominated and remineralization-dominated periods.

Short-term implication: *Following production-dominated periods, delayed peaks in CO_2 release emerge.*

6.2 Mechanistic hypotheses for carbon fixation

Carbon fixation represents the intermediate-timescale response of the coastal carbon cycle and emerges on seasonal to annual timescales through changes in biomass carbon and particulate inorganic carbon.

In EMAGIN-B.C. ver. 2, carbon fixation is governed by the balance between photosynthetic production (F) and respiratory decomposition (U) within the organic carbon pathway. In addition, $CaCO_3$ formation within the carbonate pathway contributes to the conversion of DIC into particulate inorganic carbon. Accordingly, the fixation function is governed by the dynamic balance between biological production and decomposition processes.

https://doi.org/10.5194/egusphere-2026-2710
Preprint. Discussion started: 4 June 2026

Under nutrient enrichment, multiple fixation pathways emerge depending on the relative strength of production and decomposition processes. In this study, the dominant mechanisms are classified into fixation-enhancement pathways (F1–F3) and fixation-reduction pathways (U1–U2) (**Fig. 8**).

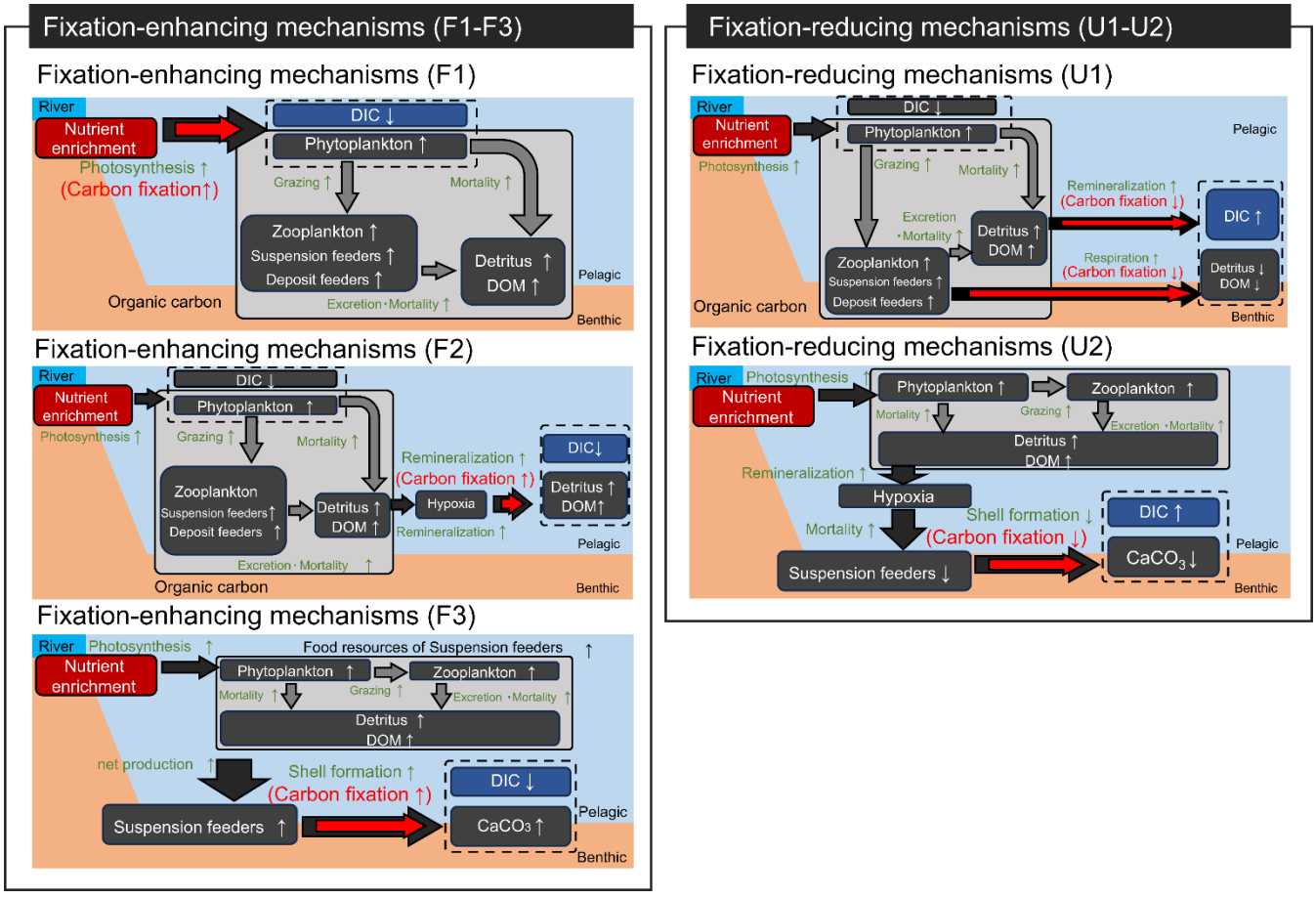

Figure 8. Conceptual diagram of the mechanisms that enhance carbon fixation (F1–F3) and those that reduce carbon fixation (U1–U2) that emerge in EMAGIN-B.C. ver. 2 under increasing nutrient loading. Each panel illustrates a causal pathway linking (i) environmental forcing (nutrient enrichment), (ii) biological and biogeochemical processes (e.g., photosynthesis, organic-matter production and sedimentation, hypoxia development, and trophic interactions), and (iii) responses of the carbonate system (e.g., DIC). The left column shows pathways that strengthen carbon fixation, whereas the right column shows pathways that weaken carbon fixation. Arrows indicate causal relationships among ecological and biogeochemical processes. Blue areas represent pelagic processes, whereas orange areas represent benthic processes. Color-coded elements indicate environmental forcing (red) and biological or biogeochemical processes (green). Upward (↑) and downward (↓) arrows denote increases and decreases in the corresponding variables or fluxes, respectively. DIC, dissolved inorganic carbon; DOM, dissolved organic matter.

https://doi.org/10.5194/egusphere-2026-2710
Preprint. Discussion started: 4 June 2026

6.2.1 Fixation-enhancement mechanisms (F-mechanisms)

(1) F1: Nutrient-stimulated pelagic primary production

An increase in nutrient supply enhances phytoplankton growth and increases the rate of photosynthetic carbon fixation. This process directly converts DIC into organic carbon biomass and strengthens the supply flux within the organic carbon pathway. As phytoplankton biomass increases, the production of particulate organic carbon also increases, which subsequently enhances the flux of organic matter toward higher trophic levels and sedimentation.

Intermediate-timescale implication: *Under moderate nutrient enrichment, pelagic primary production increases and carbon fixation is enhanced.*

(2) F2: Food-web amplification of organic carbon production

Enhanced phytoplankton production improves the food environment for zooplankton and higher trophic organisms, resulting in increased biomass throughout the food web. Through trophic transfer processes, organic carbon produced by phytoplankton is redistributed among functional groups and ultimately contributes to increased biomass carbon within the ecosystem. This mechanism constitutes a fixation pathway driven by food-web amplification within the organic carbon loop.

Intermediate-timescale implication: *When trophic transfer efficiency is high, ecosystem biomass increases, and the overall fixation capacity of the ecosystem is strengthened.*

(3) F3: $CaCO_3$ formation and particulate inorganic carbon production

In ecosystems where calcifying organisms are abundant, $CaCO_3$ formation converts DIC into particulate inorganic carbon. Although $CaCO_3$ formation releases CO_2 locally through carbonate equilibrium reactions, it simultaneously produces particulate inorganic carbon that can be transported and potentially stored in sediments. Thus, $CaCO_3$ formation constitutes an alternative pathway of carbon fixation within the carbonate loop.

Intermediate-timescale implication: *In systems dominated by calcifying organisms, carbonate production contributes to the fixation of inorganic carbon into particulate phases.*

6.2.2 Fixation-reduction mechanisms (U-mechanisms)

(1) U1: Enhanced remineralization under high organic-matter supply

When nutrient enrichment strongly enhances primary production, the supply of organic matter to the water column and sediments increases substantially. Microbial remineralization processes then intensify in response to the increased organic substrate. Through these processes, organic carbon is rapidly decomposed and returned to the DIC pool, thereby reducing net carbon fixation within the ecosystem.

https://doi.org/10.5194/egusphere-2026-2710
Preprint. Discussion started: 4 June 2026

Intermediate-timescale implication: *When remineralization rates increase faster than production rates, net fixation efficiency declines.*

(2) U2: Hypoxia-induced suppression of biological production

Under excessive nutrient loading, enhanced organic-matter decomposition can lead to severe hypoxia in bottom waters. Persistent hypoxia negatively affects benthic organisms and may also influence pelagic biological production through ecosystem instability. When ecosystem structure becomes degraded under severe hypoxia, biological production processes weaken and the fixation capacity of the ecosystem declines.

Intermediate-timescale implication: *In highly eutrophic conditions with persistent hypoxia, carbon fixation decreases despite high nutrient availability.*

6.3 Mechanistic hypotheses for carbon storage

Carbon storage represents the long-term response of the coastal carbon cycle and primarily emerges on annual to decadal timescales through the balance among sedimentation, remineralization, dissolution, and burial processes.

In EMAGIN-B.C. ver. 2, carbon storage is determined by the dynamic balance between sedimentary supply fluxes (S) and decomposition or loss fluxes (D). The supply flux consists mainly of the sedimentation of organic matter produced in the pelagic system and the downward transport of particulate inorganic carbon generated through $CaCO_3$ formation. In contrast, the loss flux includes microbial remineralization of organic matter and the dissolution of $CaCO_3$ under low-pH conditions. Accordingly, long-term carbon storage is interpreted as the residual component of the sedimentary carbon budget, determined by the relative magnitude of supply and decomposition processes. Depending on the ecosystem state and nutrient loading conditions, different storage pathways emerge. In this study, the dominant mechanisms are organised into storage-enhancement pathways (S1–S3) and storage-reduction pathways (D1–D2) (**Fig. 9**).

https://doi.org/10.5194/egusphere-2026-2710
Preprint. Discussion started: 4 June 2026

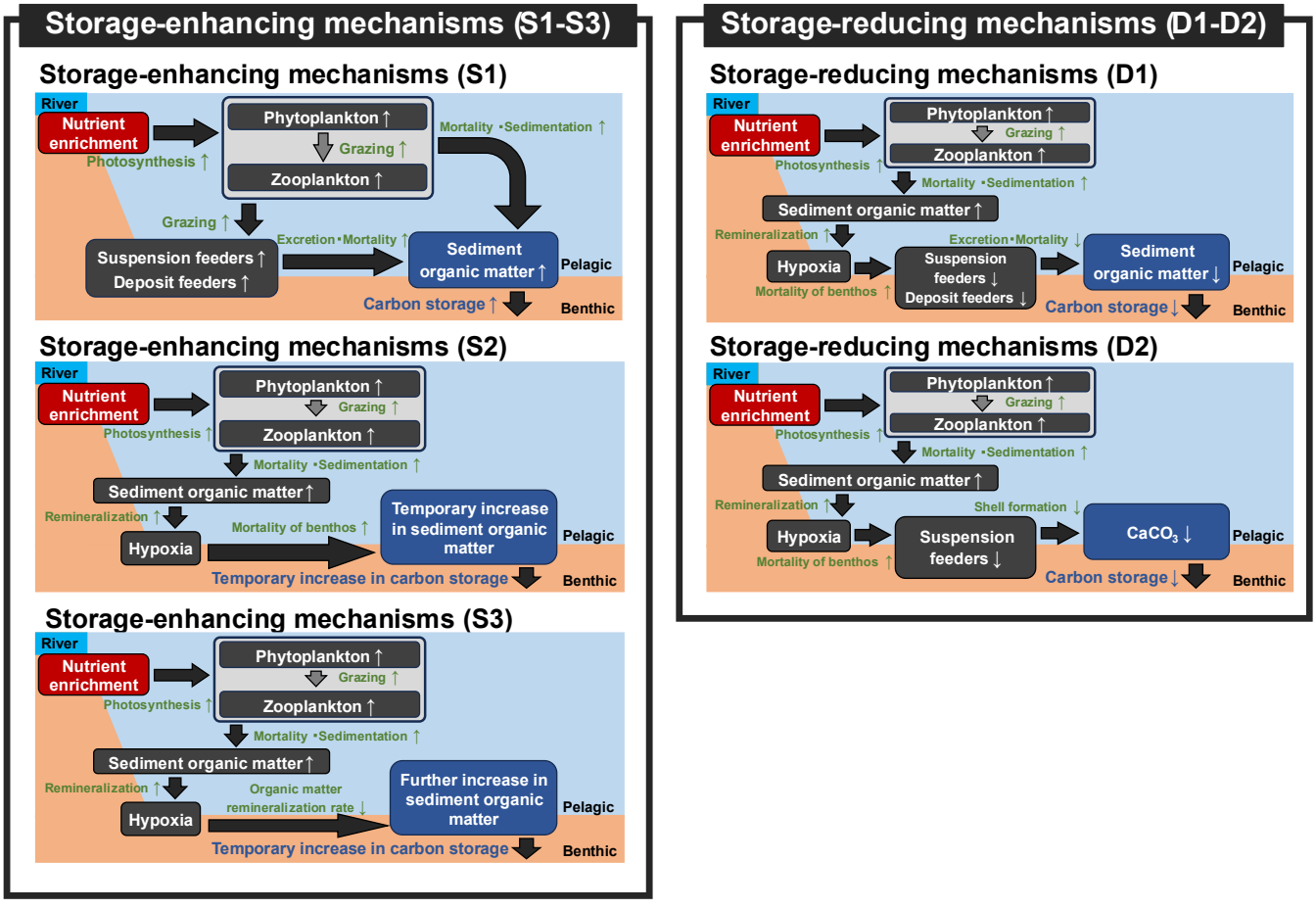

Figure 9. Conceptual diagram of carbon storage mechanisms that emerge in EMAGIN-B.C. ver. 2 under increasing nutrient loading. The left panels illustrate mechanisms that enhance carbon storage (S1–S3), whereas the right panels illustrate mechanisms that reduce carbon storage (D1–D2). Each panel represents a causal pathway linking (i) environmental forcing (nutrient enrichment), (ii) biological and biogeochemical processes (e.g., primary production, sedimentation of organic matter, hypoxia development, shell production and dissolution), and (iii) resulting changes in sedimentary carbon storage. Color-coded elements indicate environmental forcing (red), biological and biogeochemical processes (green), and carbonate or remineralization processes (blue). Blue areas represent pelagic processes, whereas orange areas represent benthic processes. Upward (↑) and downward (↓) arrows denote increases and decreases in the corresponding variables or fluxes, respectively.

6.3.1 Storage-enhancement mechanisms (S-mechanisms)

(1) S1: Enhanced burial of organic carbon through increased sedimentary supply

https://doi.org/10.5194/egusphere-2026-2710
Preprint. Discussion started: 4 June 2026

When nutrient enrichment stimulates pelagic primary production, the supply of particulate organic matter to the seabed increases via sedimentation. If the sedimentation flux exceeds the rate of microbial remineralization in sediments, a portion of the organic carbon escapes decomposition and is buried in the sediment. This mechanism constitutes a long-term storage pathway driven by enhanced organic-carbon supply from the pelagic system.

Long-term implication: *Under moderate nutrient enrichment, organic carbon burial increases through enhanced sedimentary supply.*

(2) S2: Carbon storage through $CaCO_3$ burial

Calcifying organisms produce $CaCO_3$ shells that accumulate in sediments after death. If the rate of shell production exceeds that of $CaCO_3$ dissolution, particulate inorganic carbon becomes stored in the sedimentary system. This mechanism constitutes a long-term carbon-storage pathway within the carbonate loop.

Long-term implication*: In ecosystems with abundant calcifying organisms, carbonate burial contributes substantially to long-term carbon storage.*

(3) S3: Transformation-dominated benthic carbon processing

In some coastal systems, large amounts of organic matter are laterally transported from external sources and processed by benthic organisms and microbial communities. Through this transformation process, organic carbon is redistributed within the benthic ecosystem and partially incorporated into sedimentary pools. In such systems, carbon storage occurs not only through direct pelagic production but also through the transformation and redistribution of externally supplied organic matter.

Long-term implication: *In transformation-dominated systems such as tidal flats, externally supplied organic carbon contributes significantly to sedimentary carbon storage.*

6.3.2 Storage-reduction mechanisms (D-mechanisms)

(1) D1: Enhanced remineralization exceeding sedimentary supply

When the decomposition capacity of sediments increases due to high microbial activity, remineralization exceeds the sedimentation flux of organic matter. In such cases, most of the supplied organic carbon is rapidly decomposed and returned to the DIC pool, thereby reducing long-term carbon storage.

Long-term implication: *Under conditions of strong microbial remineralization, sedimentary carbon storage remains limited even when organic-matter supply is high.*

(2) D2: Dissolution of $CaCO_3$ under low-pH conditions

https://doi.org/10.5194/egusphere-2026-2710
Preprint. Discussion started: 4 June 2026

In environments where bottom-water pH decreases due to intense remineralization or acidification processes, $CaCO_3$ dissolution intensifies within sediments. This process converts particulate inorganic carbon back into DIC and reduces long-term storage of carbonate carbon.

Long-term implication: *Under conditions of persistent low pH, carbonate storage declines due to enhanced dissolution.*

7 Spatial divergence of carbon-control structures

7.1 Overview: spatial realisation of the carbon-control framework

Sect. 6 establishes the carbon-cycle structure in EMAGIN-B.C. ver. 2 as a dual-loop system consisting of carbon uptake (A/R), carbon fixation (F/U), and carbon storage (S/D), each governed by dynamic imbalances between supply-side and loss-side fluxes across different temporal scales.

This section presents the spatial realisation of this mechanistic framework. Under a common external forcing of increased nutrient loading, the dominant processes governing these three functions are examined across three representative coastal regions: the estuarine region, central bay region, and tidal-flat region.

As shown in **Fig. 10**, all regions exhibit a common tendency, in which atmospheric CO_2 uptake and pelagic carbon fixation increase with increasing nutrient loading. This shared response reflects strengthening of supply-side processes within the organic carbon pathway, corresponding primarily to uptake mechanism A1 and fixation mechanisms F1–F2.

Process-level decomposition analyses (**Figs. 11–19**), however, show that these similar bulk responses are governed by distinct mechanistic structures across regions. The estuarine region exhibits direct amplification of supply-side fluxes within the organic carbon pathway. The central bay shows co-amplification of production and decomposition processes. The tidal-flat region exhibits a transformation-dominated structure, in which externally supplied organic carbon is redistributed and processed within the benthic system.

These differences do not simply represent variations in flux magnitude; rather, they reflect spatial differentiation in the dominant mechanisms governing carbon uptake, fixation, and storage under nutrient enrichment.

In the following sections, the relationships among A/R, F/U, and S/D are examined for each region to identify the dominant mechanisms and clarify how carbon-control structures diverge spatially.

https://doi.org/10.5194/egusphere-2026-2710
Preprint. Discussion started: 4 June 2026

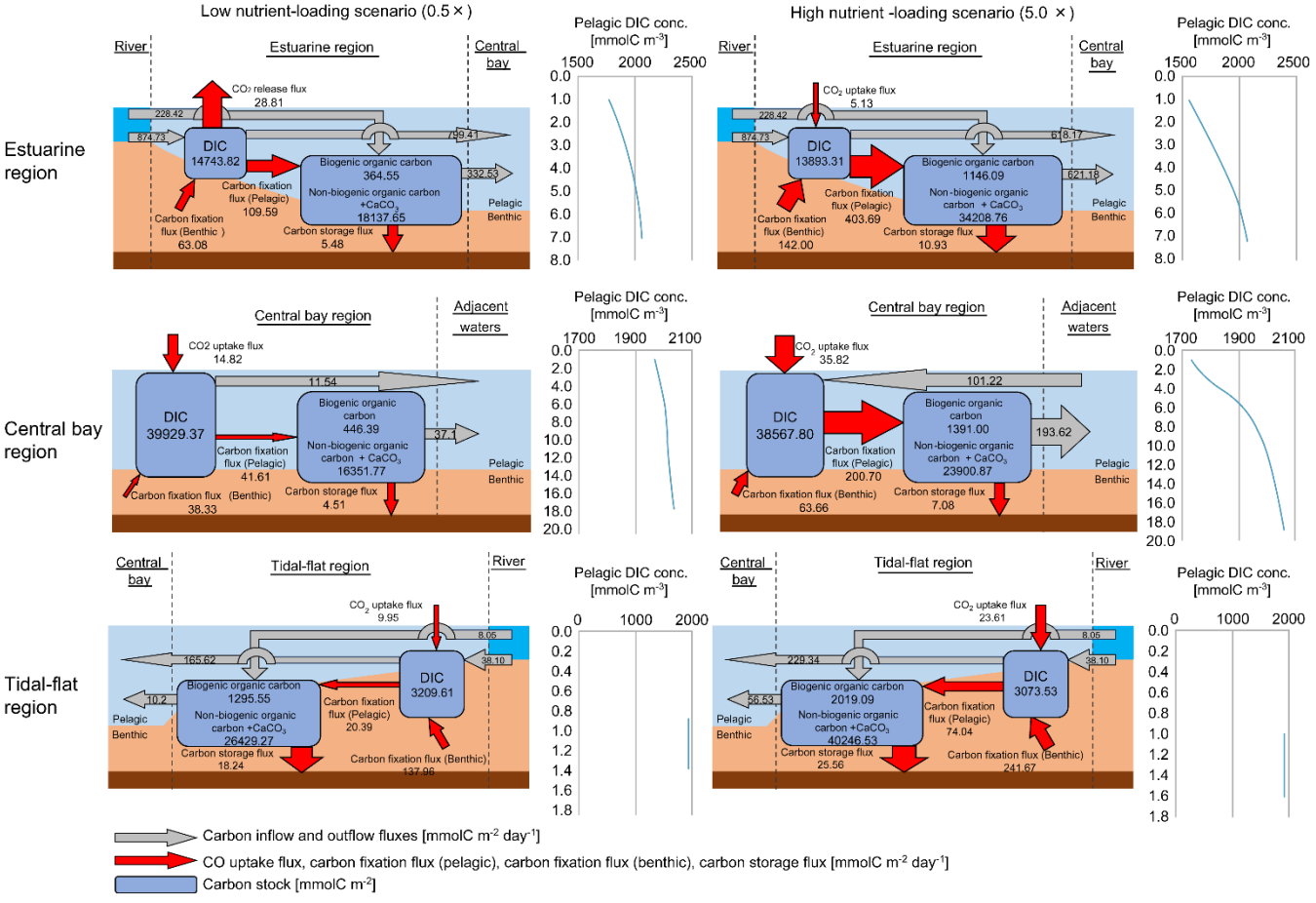

Figure 10. Process-level carbon budgets in the estuarine, central bay, and tidal-flat regions under low (0.5×) and high (5.0×) nutrient-loading scenarios relative to the control case. Blue boxes represent major carbon pools, including dissolved inorganic carbon (DIC), organic carbon, and calcium carbonate ($CaCO_3$). Arrows indicate dominant carbon fluxes such as biological production, respiration and remineralization, sedimentation, and air–sea CO_2 exchange. The diagrams illustrate how increasing nutrient loading alters the relative dominance of organic and carbonate carbon pathways, thereby defining the spatial differentiation of carbon-control structures across the three regions.

https://doi.org/10.5194/egusphere-2026-2710
Preprint. Discussion started: 4 June 2026

(i) Estuarine region

(A) Annual mean values (bars) and 1-day moving averages (lines) of air–sea CO_2 flux, carbonate-system variables, nutrients, plankton biomass, and dissolved oxygen

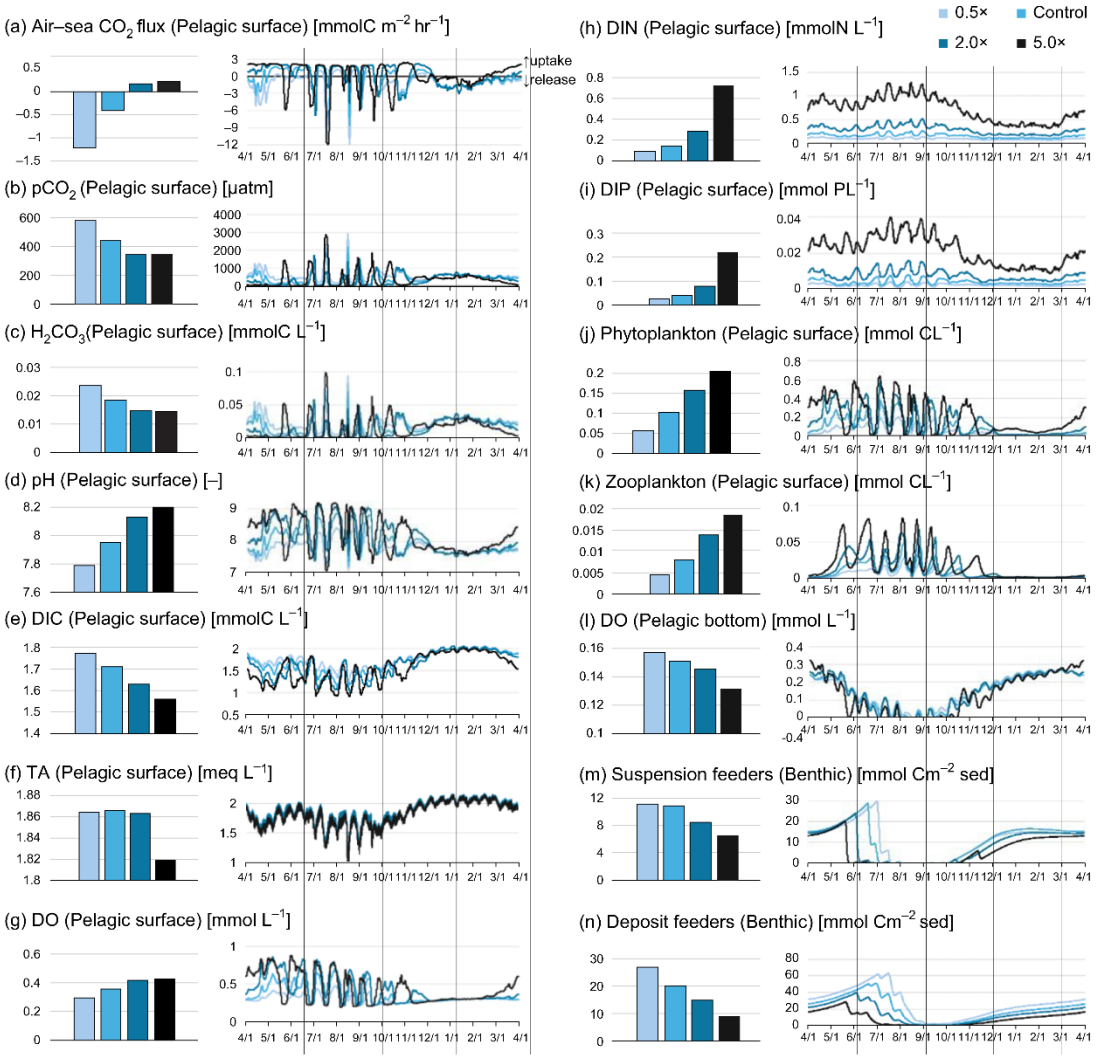

(B) Annual mean values of the production and consumption of DIC (Pelagic surface) [mmolCL^{-1} hr^{-1}]

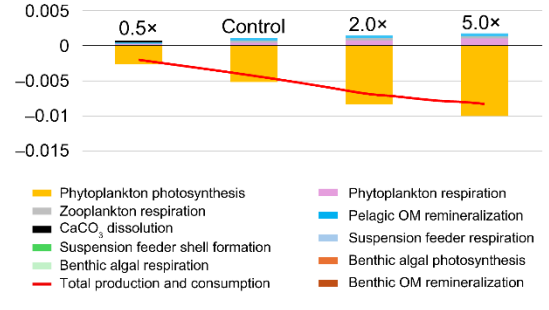

(C) Annual mean values of the production and consumption of TA (Pelagic surface) [meq L^{-1} hr^{-1}]

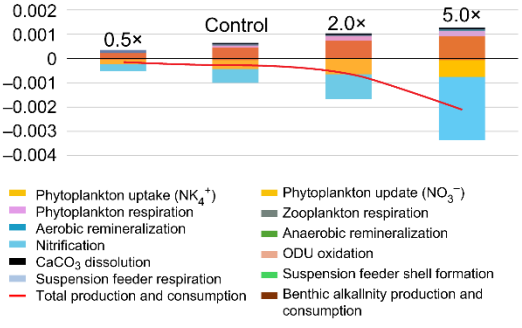

https://doi.org/10.5194/egusphere-2026-2710
Preprint. Discussion started: 4 June 2026

Figure 11. Responses of atmospheric CO_2 uptake and carbonate-system variables in the estuarine region under different nutrient-loading scenarios (0.5×, 1.0× [control], 2.0×, and 5.0×). (A) Annual mean values (bars) and seasonal variations represented by 1-day moving averages (lines) of air–sea CO_2 flux, carbonate-system variables (pCO_2, H_2CO_3, pH, DIC, and TA), nutrients (DIN and DIP), plankton biomass, and DO. (B) Annual mean values of DIC production and consumption fluxes. (C) Annual mean values of TA production and consumption fluxes. These panels illustrate the mechanisms controlling carbon uptake (A/R), corresponding to the imbalance between air–sea CO_2 uptake and respiratory CO_2 release and reflecting the uptake and release pathways (A1–A3 and R1–R3) defined in Sect. 6.1. DIC, dissolved inorganic carbon; DIN, dissolved inorganic nitrogen; DIP, dissolved inorganic phosphorus; DO, dissolved oxygen; TA, total alkalinity.

https://doi.org/10.5194/egusphere-2026-2710
Preprint. Discussion started: 4 June 2026

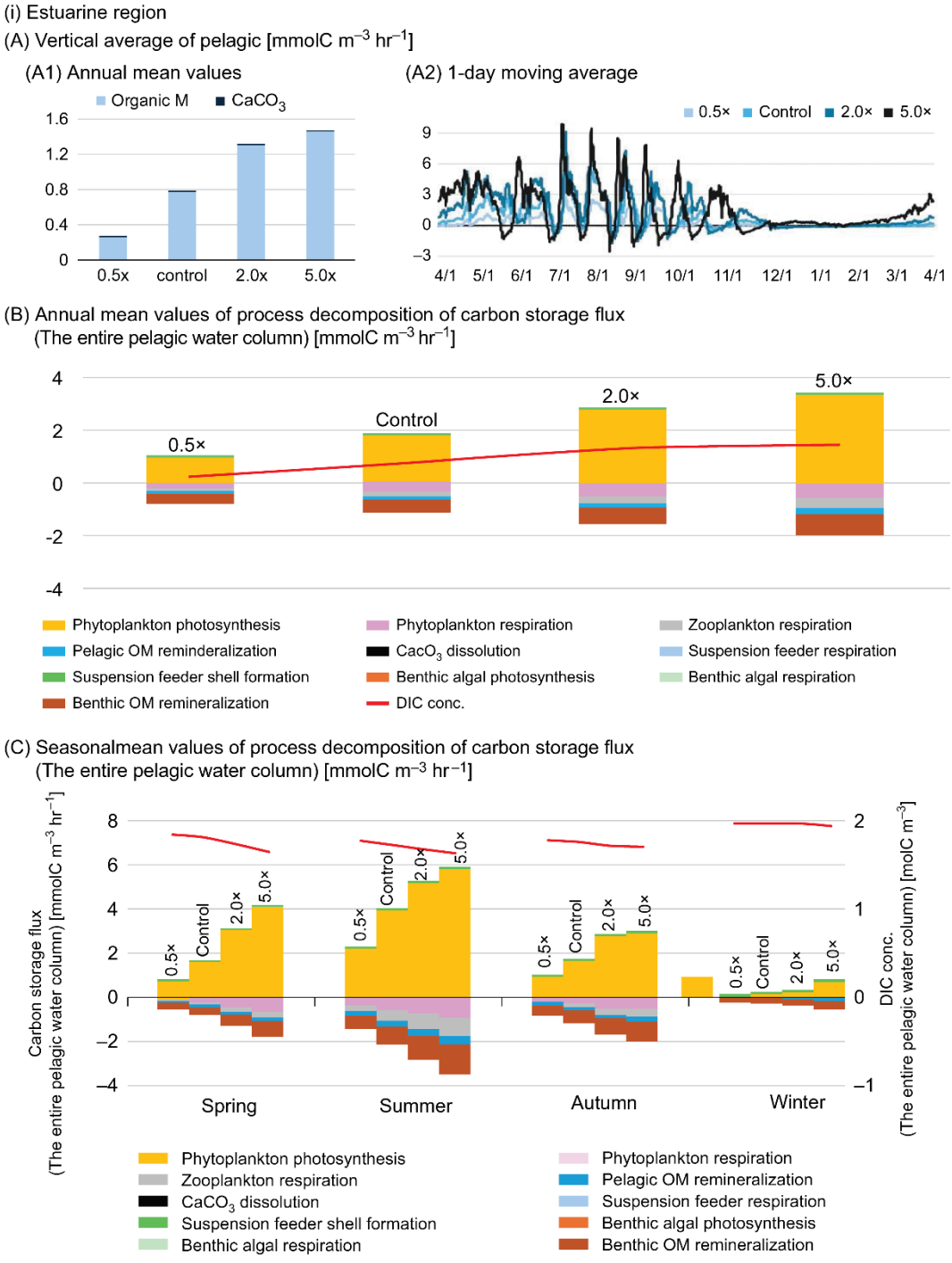

580 **Figure 12. Responses of carbon fixation processes in the estuarine region under different nutrient-loading scenarios (0.5×, control, 2.0×, and 5.0×). (A) Vertically averaged carbon fixation fluxes represented as annual mean values (bars) and seasonal variations shown by 1-day moving averages (lines). (B) Annual mean values of the major carbon fixation and respiration processes, including**

https://doi.org/10.5194/egusphere-2026-2710
Preprint. Discussion started: 4 June 2026

phytoplankton photosynthesis and respiration. (C) Seasonal variations of the major carbon fixation and respiration processes. These panels illustrate the mechanisms controlling carbon fixation (F/U), corresponding to the balance between photosynthetic production and respiratory decomposition and reflecting the fixation-enhancement and reduction pathways (F1–F3 and U1–U2) defined in Sect. 6.2. Coloured bars distinguish organic carbon processes and calcium carbonate processes.

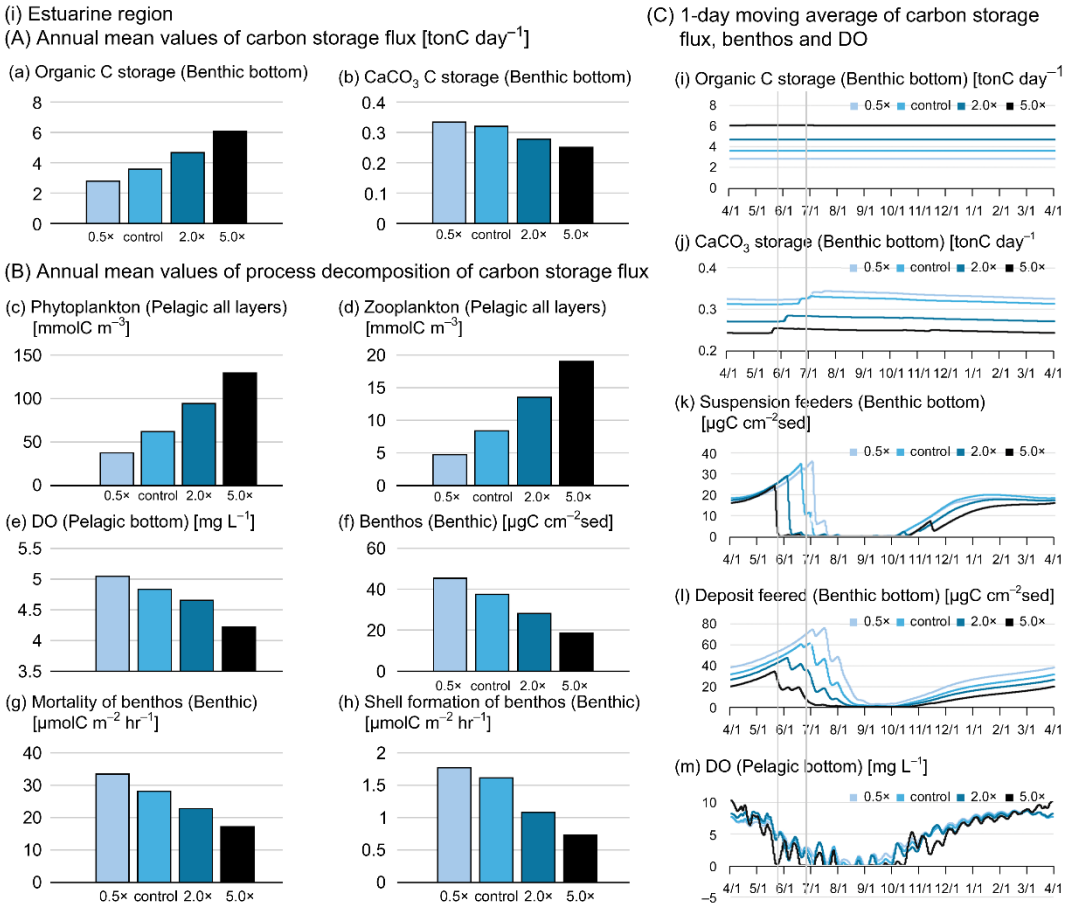

Figure 13. Responses of carbon storage processes in the estuarine region under different nutrient-loading scenarios (0.5×, control, 2.0×, and 5.0×). (A) Annual fluxes of sedimentary organic carbon storage and $CaCO_3$ storage. (B) Process decomposition of sedimentary carbon supply and decomposition fluxes contributing to carbon storage. (C) Time series of benthic organic matter, $CaCO_3$ stocks, benthic-faunal biomass, and bottom-layer dissolved oxygen (DO), shown as 1-day moving averages. These panels illustrate the mechanisms controlling carbon storage (S/D), corresponding to the balance between sedimentary carbon supply and decomposition processes and reflecting the storage-enhancement and reduction pathways (S1–S3 and D1–D2) defined in Sect. 6.3. Benthic fauna (benthos) is defined as the sum of suspension feeders and deposit feeders.

https://doi.org/10.5194/egusphere-2026-2710
Preprint. Discussion started: 4 June 2026

(ii) Central bay

(A) Annual mean values (bars) and 1-day moving averages (lines) of air–sea CO_2 flux carbonate-system variables, nutrients, plankton biomass, and dissolved oxygen,

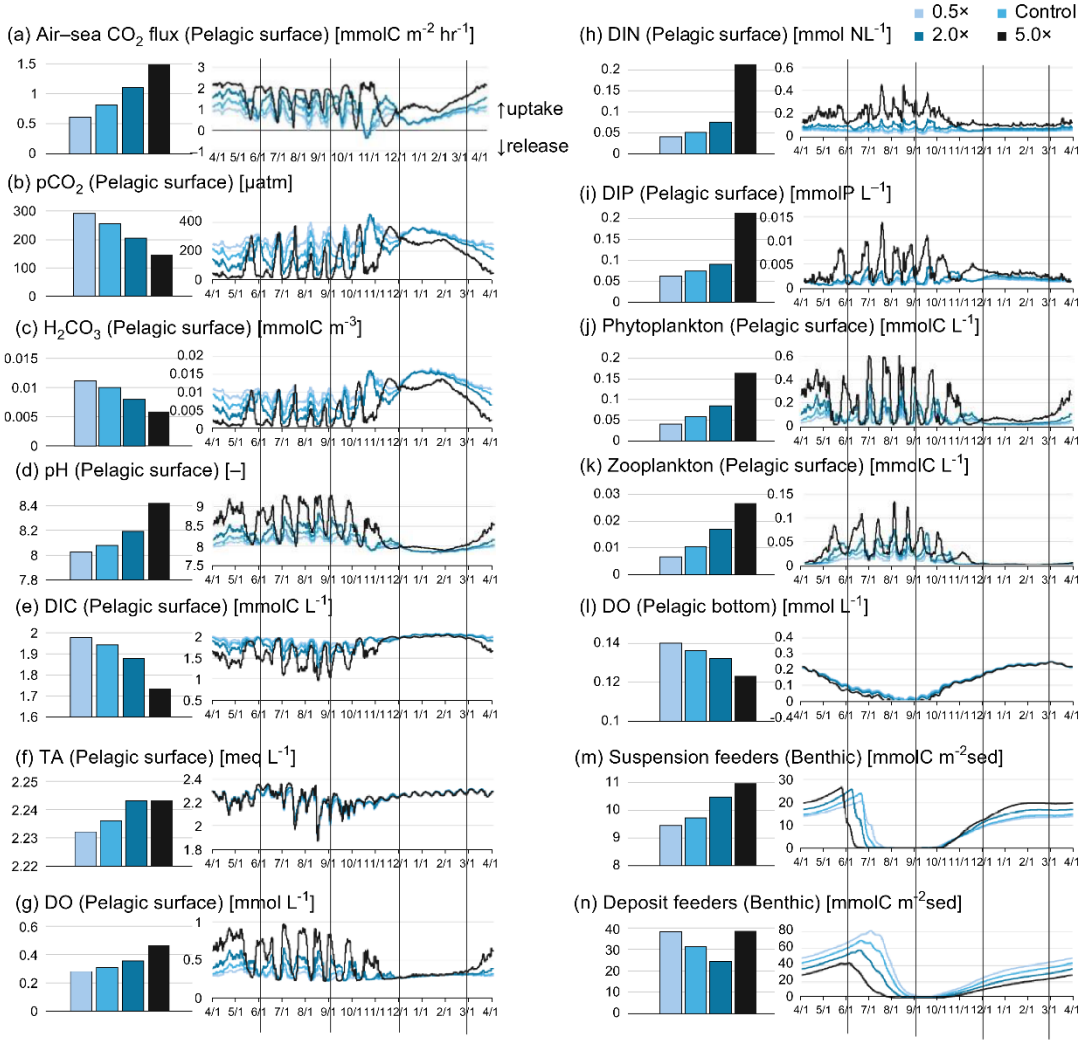

(B) Annual mean values of the production and consumption of DIC (Pelagic surface) [mmolC L^{-1} hr^{-1}]

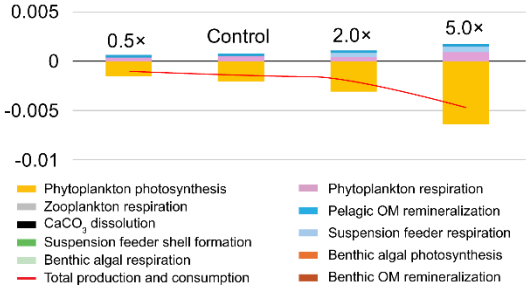

(C) Annual mean values of the production and consumption of TA (Pelagic surface) [meq L^{-1} hr^{-1}]

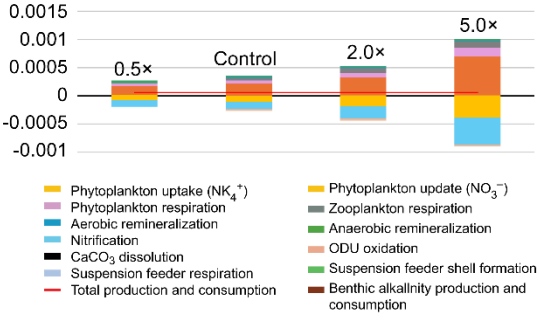

595

https://doi.org/10.5194/egusphere-2026-2710
Preprint. Discussion started: 4 June 2026

Figure 14. Responses of atmospheric CO_2 uptake and carbonate-system variables in the central bay region under different nutrient-loading scenarios (0.5×, 1.0× [control], 2.0×, and 5.0×). (A) Annual mean values (bars) and seasonal variations represented by 1-day moving averages (lines) of air–sea CO_2 flux, carbonate-system variables (pCO_2, H_2CO_3, pH, DIC, and TA), nutrients (DIN and DIP), plankton biomass, and DO. (B) Annual mean values of DIC production and consumption fluxes. (C) Annual mean values of TA production and consumption fluxes. These panels illustrate the mechanisms controlling carbon uptake (A/R), corresponding to the imbalance between air–sea CO_2 uptake and respiratory CO_2 release and reflecting the uptake and release pathways (A1–A3 and R1–R3) defined in Sect. 6.1. DIC, dissolved inorganic carbon; DIN, dissolved inorganic nitrogen; DIP, dissolved inorganic phosphorus; DO, dissolved oxygen; TA, total alkalinity.

https://doi.org/10.5194/egusphere-2026-2710
Preprint. Discussion started: 4 June 2026

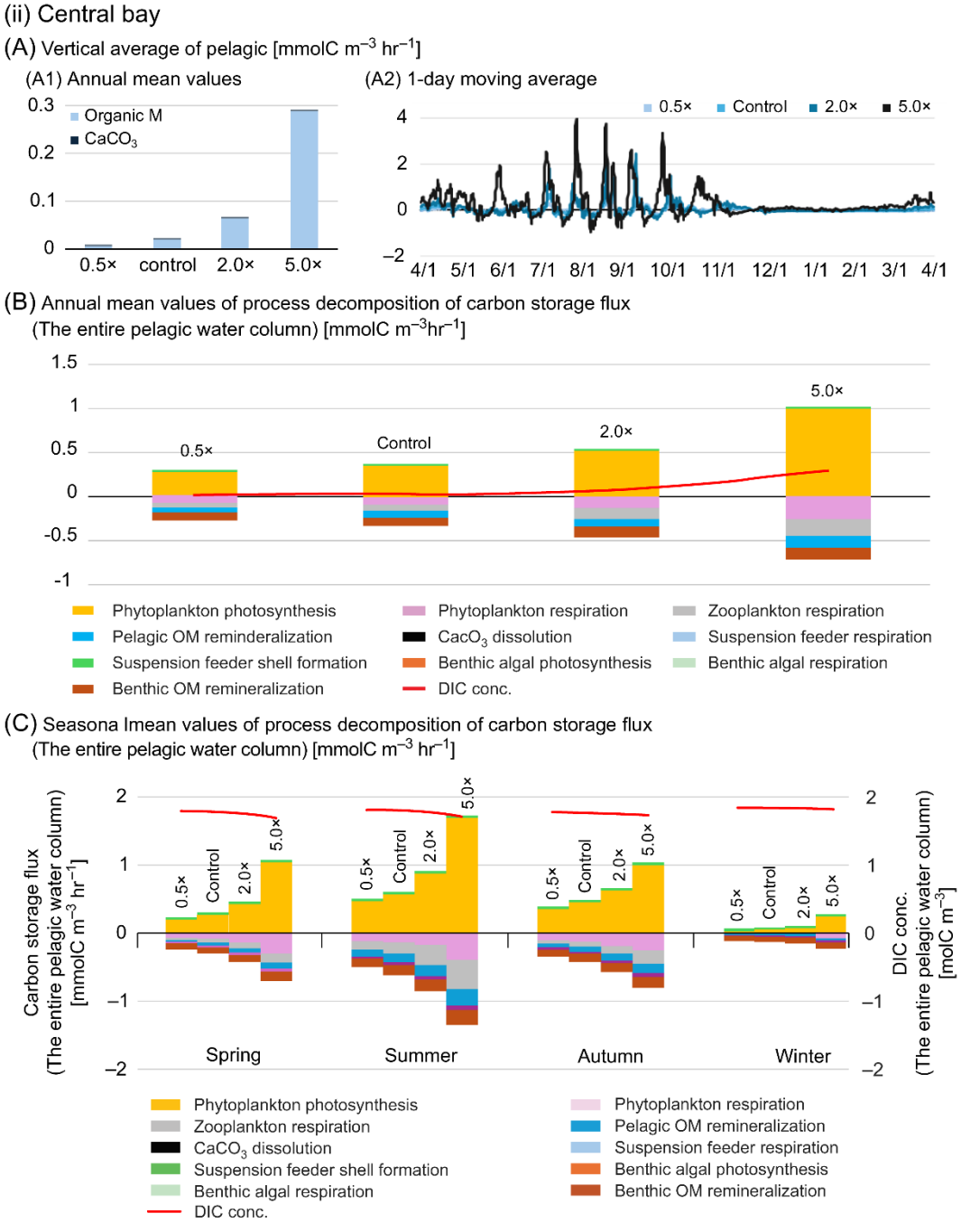

Figure 15. Responses of carbon fixation processes in the central bay region under different nutrient-loading scenarios (0.5×, control, 2.0×, and 5.0×). (A) Vertically averaged carbon fixation fluxes represented as annual mean values (bars) and seasonal variations shown by 1-day moving averages (lines). (B) Annual mean values of the major carbon fixation and respiration processes, including phytoplankton photosynthesis and respiration. (C) Seasonal variations of the major carbon fixation and respiration

https://doi.org/10.5194/egusphere-2026-2710
Preprint. Discussion started: 4 June 2026

processes. These panels illustrate the mechanisms controlling carbon fixation (F/U), corresponding to the balance between photosynthetic production and respiratory decomposition and reflecting the fixation-enhancement and reduction pathways (F1–F3 and U1–U2) defined in Sect. 6.2.

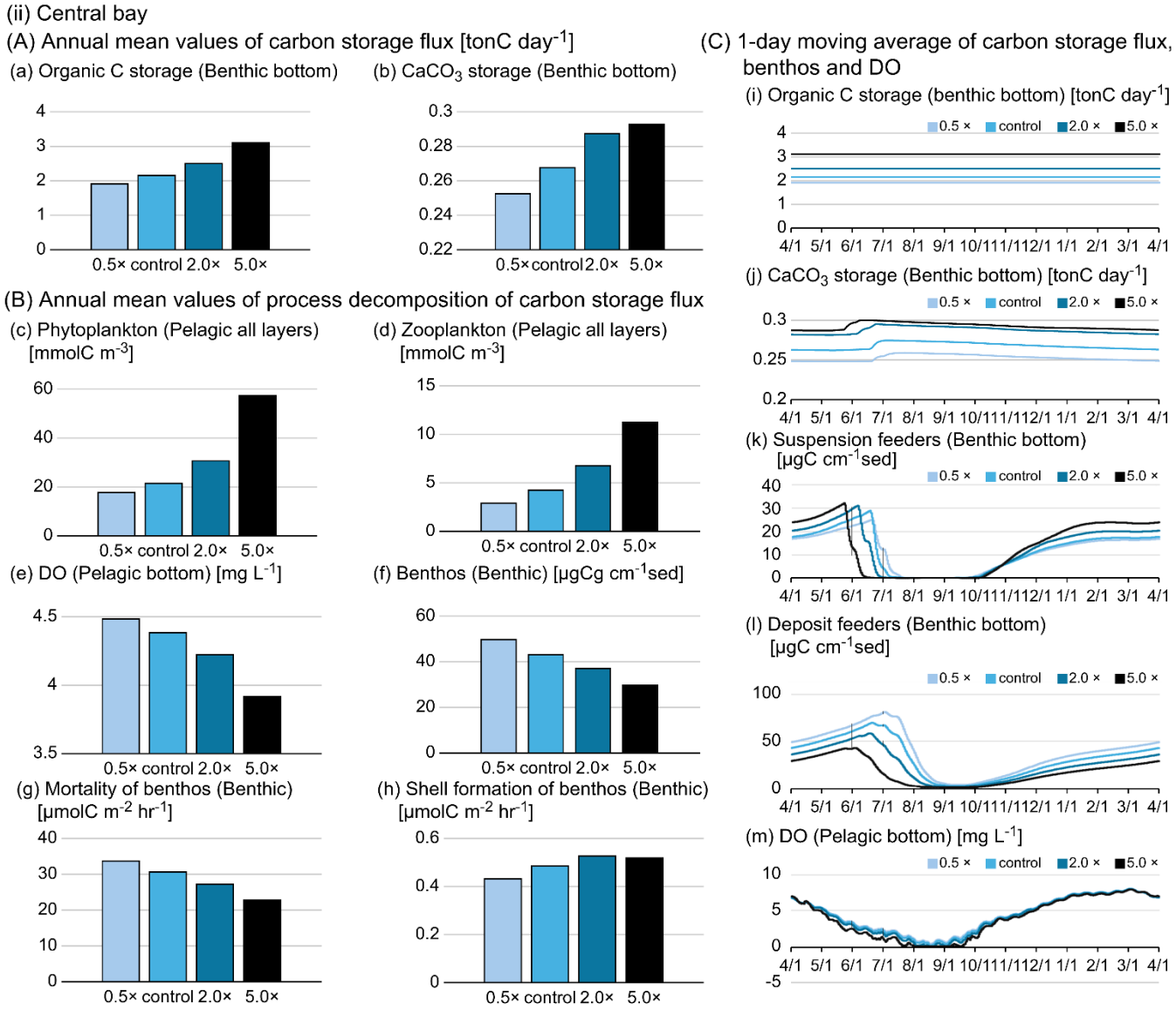

Figure 16. Responses of carbon storage processes in the central bay region under different nutrient-loading scenarios (0.5×, control, 2.0×, and 5.0×). (A) Annual fluxes of sedimentary organic carbon storage and $CaCO_3$ storage. (B) Process decomposition of sedimentary carbon supply and decomposition fluxes contributing to carbon storage. (C) Time series of benthic organic matter, $CaCO_3$ stocks, benthic-faunal biomass, and bottom-layer dissolved oxygen (DO), shown as 1-day moving averages. These panels illustrate the mechanisms controlling carbon storage (S/D), corresponding to the balance between sedimentary carbon supply and

https://doi.org/10.5194/egusphere-2026-2710
Preprint. Discussion started: 4 June 2026

decomposition processes and reflecting the storage-enhancement and reduction pathways (S1–S3 and D1–D2) defined in Sect. 6.3. Benthic fauna (benthos) is defined as the sum of suspension feeders and deposit feeders.

https://doi.org/10.5194/egusphere-2026-2710
Preprint. Discussion started: 4 June 2026

(iii) Tidal-flat system

(A) Annual mean values (bars) and 1-day moving averages (lines) of air–sea CO_2 flux, carbonate-system variables, nutrients, plankton biomass, and dissolved oxygen

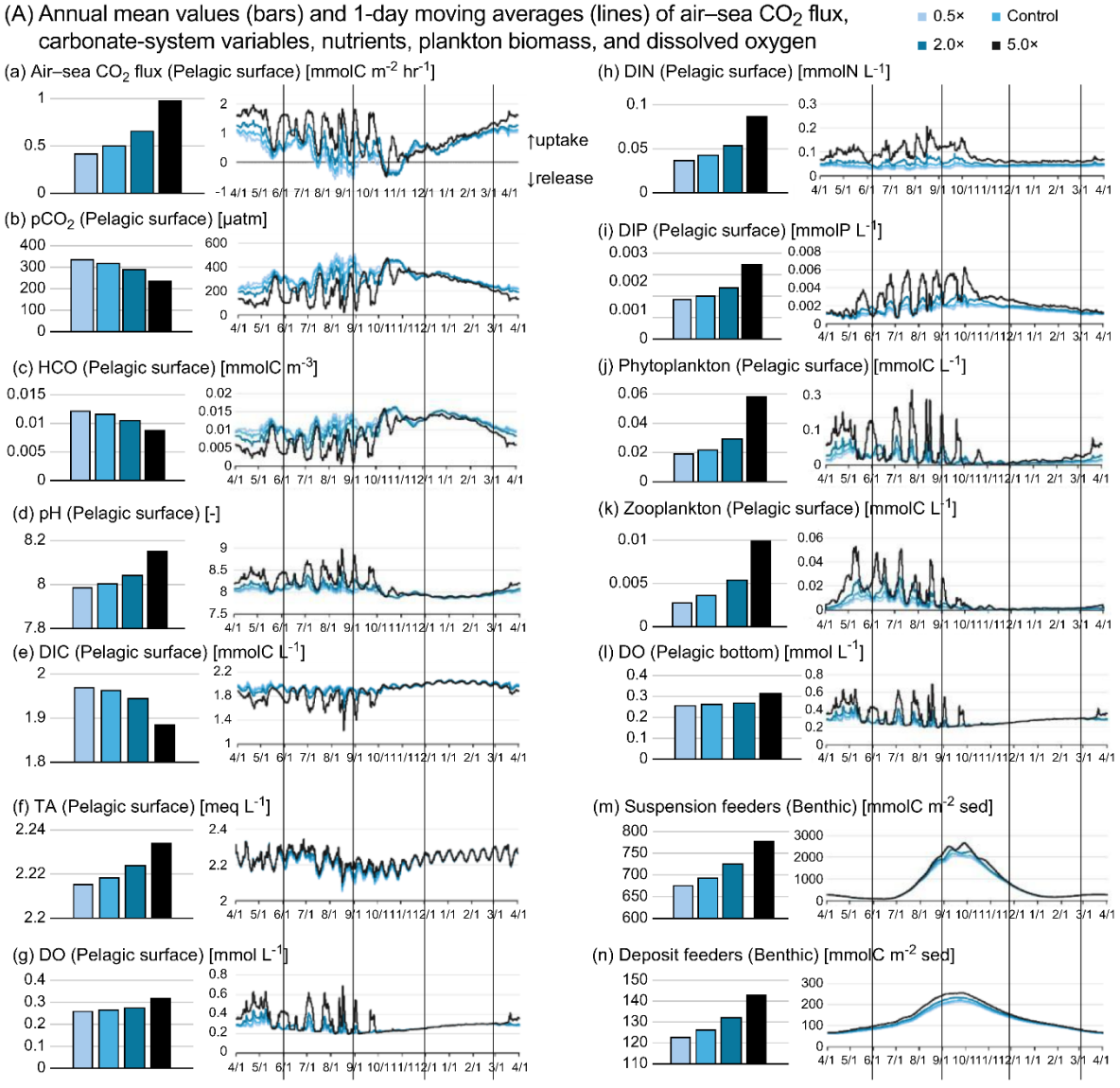

(B) Annual mean values of the production and consumption of DIC (Pelagic surface) [mmolC L^{-1} hr^{-1}]

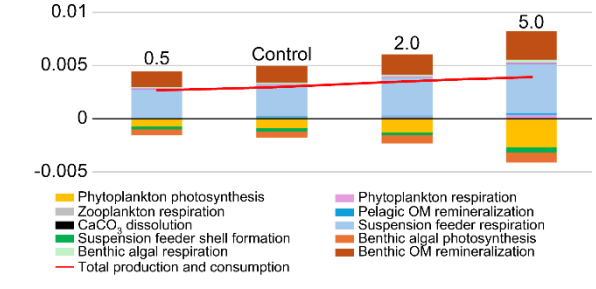

(C) Annual mean values of the production and consumption of TA (Pelagic surface) [meq L^{-1} hr^{-1}]

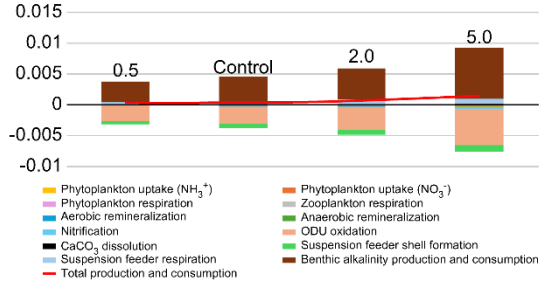

https://doi.org/10.5194/egusphere-2026-2710
Preprint. Discussion started: 4 June 2026

Figure 17. Responses of atmospheric CO_2 uptake and carbonate-system variables in the tidal-flat region under different nutrient-loading scenarios (0.5×, control, 2.0×, and 5.0×). (A) Annual mean values (bars) and seasonal variations represented by 1-day moving averages (lines) of air–sea CO_2 flux, carbonate-system variables (pCO_2, H_2CO_3, pH, DIC, and TA), nutrients (DIN and DIP), plankton biomass, and DO. (B) Annual mean values of DIC production and consumption fluxes. (C) Annual mean values of TA production and consumption fluxes. These panels illustrate the mechanisms controlling carbon uptake (A/R), corresponding to the imbalance between air–sea CO_2 uptake and respiratory CO_2 release and reflecting the uptake and release pathways (A1–A3 and R1–R3) defined in Sect. 6.1. DIC, dissolved inorganic carbon; DIN, dissolved inorganic nitrogen; DIP, dissolved inorganic phosphorus; DO, dissolved oxygen; TA, total alkalinity.

https://doi.org/10.5194/egusphere-2026-2710
Preprint. Discussion started: 4 June 2026

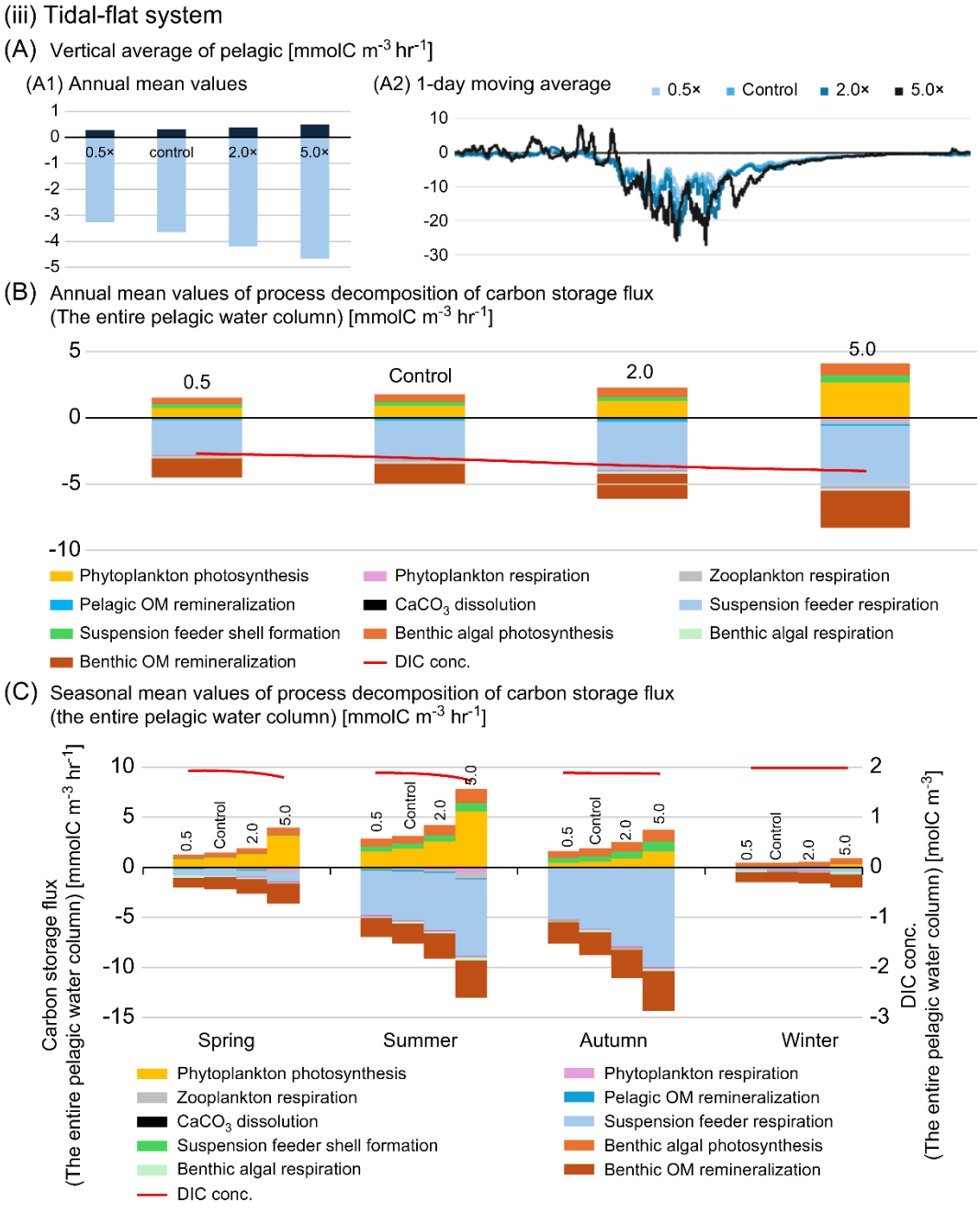

Figure 18. Responses of carbon fixation processes in the tidal-flat region under different nutrient-loading scenarios (0.5×, control, 2.0×, and 5.0×). (A) Vertically averaged carbon fixation fluxes represented as annual mean values (bars) and seasonal variations shown by 1-day moving averages (lines). (B) Annual mean values of the major carbon fixation and respiration processes, including phytoplankton photosynthesis and respiration. (C) Seasonal variations of the major carbon fixation and respiration processes. These panels illustrate the mechanisms controlling carbon fixation (F/U), corresponding to the balance between photosynthetic

https://doi.org/10.5194/egusphere-2026-2710
Preprint. Discussion started: 4 June 2026

production and respiratory decomposition and reflecting the fixation-enhancement and reduction pathways (F1–F3 and U1–U2) defined in Sect. 6.2.

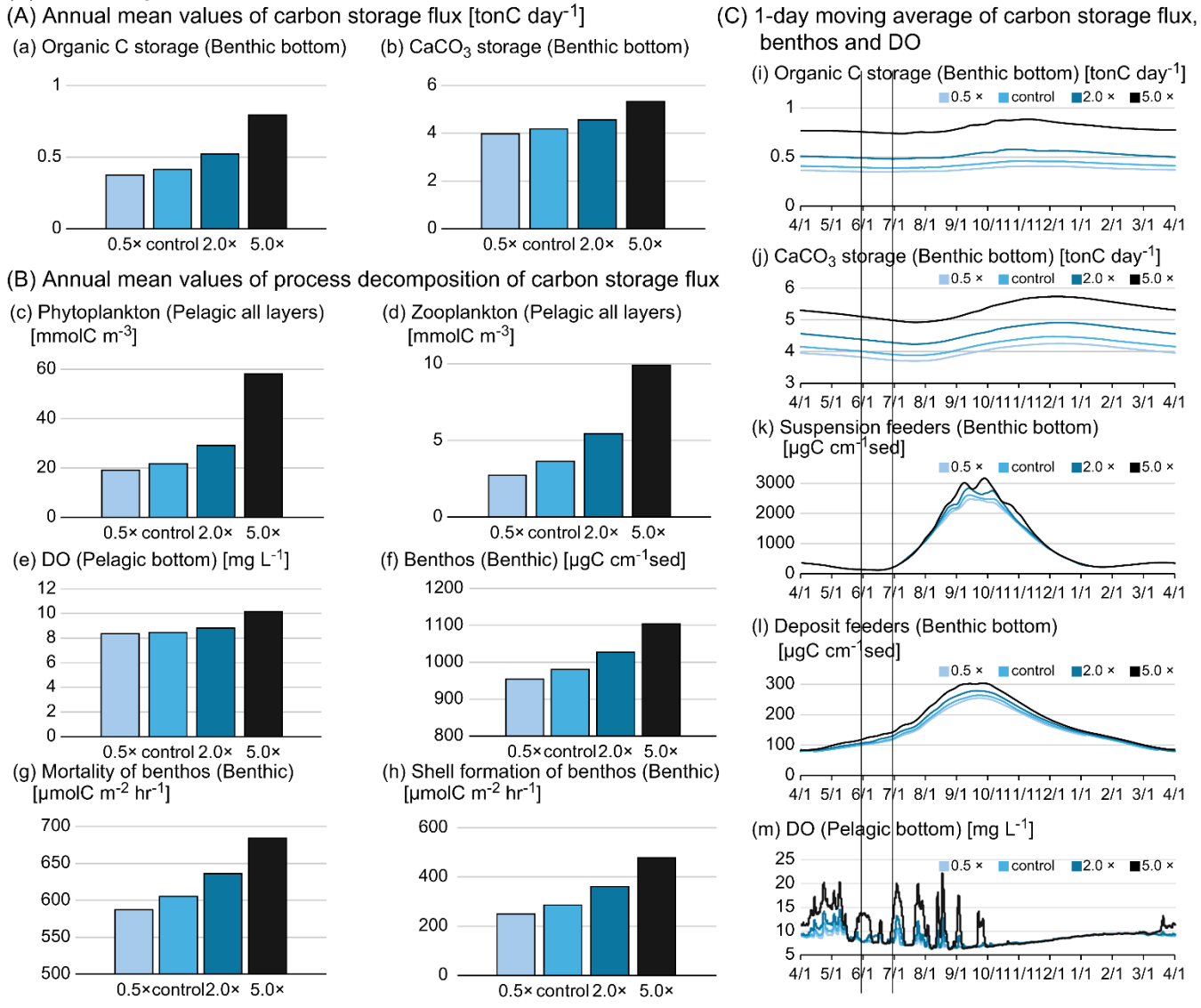

Figure 19. Responses of carbon storage processes in the tidal-flat region under different nutrient-loading scenarios (0.5×, control, 2.0×, and 5.0×). (A) Annual fluxes of sedimentary organic carbon storage and $CaCO_3$ storage. (B) Process decomposition of sedimentary carbon supply and decomposition fluxes contributing to carbon storage. (C) Time series of benthic organic matter, $CaCO_3$ stocks, benthic-faunal biomass, and bottom-layer dissolved oxygen (DO), shown as 1-day moving averages. These panels illustrate the mechanisms controlling carbon storage (S/D), corresponding to the balance between sedimentary carbon supply and

https://doi.org/10.5194/egusphere-2026-2710
Preprint. Discussion started: 4 June 2026

decomposition processes and reflecting the storage-enhancement and reduction pathways (S1–S3 and D1–D2) defined in Sect. 6.3. Benthic fauna (benthos) is defined as the sum of suspension feeders and deposit feeders.

7.2 Estuarine region: pelagic amplification response — monotonic amplification type

7.2.1 Response of carbon uptake (A/R)

As shown in **Fig. 11**, the air–sea CO_2 uptake flux in the estuarine region increases monotonically with increasing nutrient loading. This pattern is explained by the amplification of pelagic photosynthesis, which enhances DIC consumption, reduces surface-water pCO_2, and thereby drives atmospheric CO_2 uptake. This response corresponds primarily to the pelagic photosynthetic drawdown mechanism (A1) defined in **Sect. 6.1**.

Although remineralization (U) also increases, its rate of increase does not exceed that of photosynthetic production. As a result, the net DIC balance remains dominated by consumption processes, and no shift toward release-dominated conditions is observed. In this sense, the contribution of release pathways (R1–R3) remains limited.

Accordingly, the A/R structure in the estuarine region constitutes a monotonic amplification regime dominated by supply-side processes within the organic carbon pathway.

7.2.2 Response of carbon fixation (F/U)

As shown in **Fig. 12(A)**, carbon fixation increases with increasing nutrient loading. This increase is explained by the strengthening of pelagic primary production, corresponding to the nutrient-stimulated production pathway (F1) defined in **Sect. 6.2**.

However, it is necessary to distinguish between fixation flux and the resulting accumulation of fixed carbon. While fixation flux (i.e., production rate) increases, the annual mean biomass of benthic fauna decreases (**Fig. 13**), and seasonal patterns indicate that mortality of suspension feeders and deposit feeders increases during the summer hypoxic period, with an extended duration under higher nutrient-loading conditions. These responses reflect the concurrent intensification of decomposition and oxygen-limitation-related loss processes, corresponding to remineralization-driven reduction (U1) and hypoxia-induced suppression (U2).

Despite this co-amplification of production and loss processes, net fixation continues to increase monotonically, and the F–U difference remains positive across the loading scenarios. This indicates that production processes consistently exceed decomposition processes.

Accordingly, the F/U relationship in the estuarine region constitutes a non-competitive regime dominated by fixation-enhancement pathways, in which the increase in F1 is not offset by U1–U2.

https://doi.org/10.5194/egusphere-2026-2710
Preprint. Discussion started: 4 June 2026

7.2.3 Response of carbon storage (S/D)

As shown in **Fig. 13**, organic carbon storage increases with increasing nutrient loading, whereas $CaCO_3$ storage exhibits a decreasing tendency. This pattern reflects the enhancement of organic-matter supply and burial processes, corresponding to the storage-enhancement pathway (S1) defined in **Sect. 6.3**.

The decrease in $CaCO_3$ storage corresponds to the reduction in benthic-faunal biomass, which limits shell production and thus reduces the particulate inorganic carbon supply. This response reflects a weakening of the carbonate-associated storage pathway (S2).

Accordingly, in the estuarine region, carbon storage is increasingly dominated by organic-matter pathways, while carbonate supply remains limited, and no pronounced amplification of dissolution (D1–D2) is observed.

Therefore, the S/D structure in the estuarine region constitutes an organic-matter-dominated storage regime, in which S1 is enhanced, while S2 is suppressed and loss processes remain secondary.

7.2.4 Summary of the estuarine response

The estuarine region is summarised as follows:

- Uptake: a monotonic amplification pattern dominated by pelagic photosynthetic drawdown (A1), with limited contribution from release pathways (R1–R3);
- Fixation: a non-competitive structure in which fixation-enhancement pathways (F1–F3) exceed decomposition pathways (U1–U2), and the F–U difference remains positive;
- Storage: an organic-matter-dominated structure characterised by the enhancement of organic carbon burial (S1) and suppression of carbonate-associated storage (S2), with limited contribution from loss pathways (D1–D2).

Accordingly, under increased nutrient loading, the estuarine region is governed by pelagic amplification within the organic carbon pathway, without transition to an alternative carbon-control structure.

7.3 Central bay region: production–decomposition amplification response — co-amplification type

7.3.1 Response of carbon uptake (A/R)

As shown in **Fig. 14**, the air–sea CO_2 uptake flux in the central bay increases with increasing nutrient loading. This increase is explained by the enhancement of pelagic photosynthesis in the surface layer, which promotes DIC consumption and corresponds to the pelagic photosynthetic drawdown mechanism (A1) defined in **Sect. 6.1**.

In contrast to the estuarine region, remineralization in the bottom layer is also strongly amplified. As shown in **Fig. 14**, remineralization-related fluxes increase substantially with nutrient loading, and bottom-layer DIC concentration increases,

https://doi.org/10.5194/egusphere-2026-2710
Preprint. Discussion started: 4 June 2026

reflecting enhanced decomposition processes corresponding to remineralization-driven pathways (U1) and post-production DIC accumulation (R3).

Accordingly, the central bay exhibits a vertically differentiated structure in which surface-layer CO_2 uptake is driven by enhanced photosynthesis (A1), while bottom-layer DIC regeneration is intensified by decomposition processes (U1 and R3). As a result, although atmospheric CO_2 uptake increases overall, the A/R structure does not constitute an F-dominated monotonic amplification pattern; instead, it constitutes a co-amplification regime in which both supply-side (A1) and loss-side (R3) processes are simultaneously intensified.

7.3.2 Response of carbon fixation (F/U)

As shown in **Fig. 15(A)**, carbon fixation flux increases markedly with increasing nutrient loading. This increase is explained by the strengthening of pelagic primary production, corresponding to the nutrient-stimulated production pathway (F1) defined in **Sect. 6.2**. The magnitude of this increase under the 2.0×–5.0× loading scenarios exceeds that observed in the estuarine region.

At the same time, remineralization is also strongly amplified. As shown in **Fig. 14**, decomposition-related fluxes increase substantially with nutrient loading, and benthic-faunal dynamics (**Fig. 16**) indicate seasonal biomass increases during the spring–autumn growth period, followed by enhanced mortality during the summer hypoxic period, with an extended duration under higher nutrient-loading conditions. These responses reflect the intensification of decomposition and oxygen-limitation-related loss processes, corresponding to remineralization-driven reduction (U1) and hypoxia-induced suppression (U2).

Accordingly, nutrient enrichment simultaneously enhances production (F1) and decomposition (U1–U2), resulting in a coupled amplification of both processes. Consequently, the F–U difference does not increase monotonically but varies depending on the relative strength of these competing pathways.

In contrast to the estuarine region, where fixation remains dominated by production processes, the central bay exhibits a strongly coupled F/U structure in which production and decomposition are co-amplified.

Thus, the F/U relationship in the central bay constitutes a co-amplification regime in which fixation-enhancement (F1–F3) and reduction pathways (U1–U2) are simultaneously intensified.

7.3.3 Response of carbon storage (S/D)

As shown in **Fig. 16**, organic carbon storage increases with increasing nutrient loading. This increase reflects the enhancement of organic-matter supply and burial processes, corresponding to the storage-enhancement pathway (S1) defined in **Sect. 6.3**.

https://doi.org/10.5194/egusphere-2026-2710
Preprint. Discussion started: 4 June 2026

In contrast to the estuarine region, $CaCO_3$ storage also increases. This increase reflects the combined effects of enhanced suspension-feeder biomass during the growth period and the persistence of shell material following summer mortality events, corresponding to an intensification of the carbonate-associated storage pathway (S2).

Accordingly, nutrient enrichment enhances biological production and subsequently amplifies mortality-driven shell supply to the sediment, resulting in increased particulate inorganic carbon accumulation. This behaviour indicates that both organic (S1) and carbonate (S2) storage pathways are simultaneously strengthened.

Therefore, the S/D structure in the central bay constitutes a co-amplification regime in which increases in organic matter and $CaCO_3$ storage coexist, whereas loss processes (D1–D2) remain subordinate.

7.3.4 Summary of the central bay response

The central bay region is summarised as follows:

- Uptake: a co-amplification structure in which pelagic photosynthetic drawdown (A1) and decomposition-driven pathways (R3) are simultaneously intensified;
- Fixation: a strongly coupled F/U structure in which fixation-enhancement pathways (F1–F3) and reduction pathways (U1–U2) are co-amplified, and the net fixation (F–U) varies depending on nutrient loading;
- Storage: a co-amplification structure in which both organic carbon burial (S1) and carbonate-associated storage (S2) increase, while loss pathways (D1–D2) remain secondary.

Accordingly, nutrient enrichment in the central bay strengthens the coupling of internal ecosystem processes by simultaneously enhancing production and decomposition across both organic and carbonate pathways.

In contrast to the pelagic-dominated monotonic amplification regime of the estuarine region, the central bay constitutes a co-amplification regime in which supply-side and loss-side processes are simultaneously intensified.

7.4 Tidal-flat region: transformation-dominated regime

7.4.1 Response of carbon uptake (A/R)

As shown in **Fig. 17**, the air–sea CO_2 uptake flux in the tidal-flat region increases with increasing nutrient loading. This increase is explained by enhanced pelagic primary production, which promotes DIC consumption in the surface water and corresponds to the pelagic photosynthetic drawdown mechanism (A1) defined in **Sect. 6.1**.

However, the magnitude of the increase in CO_2 uptake is smaller than that observed in the estuarine and central bay regions. This difference reflects the stronger influence of benthic processes in the tidal-flat region.

https://doi.org/10.5194/egusphere-2026-2710
Preprint. Discussion started: 4 June 2026

In the tidal-flat region, a substantial fraction of organic matter supplied from the water column is transported to the sediment, where it undergoes intensive decomposition and transformation processes. These processes enhance benthic remineralization and DIC regeneration, corresponding to decomposition-driven pathways (U1) and post-production accumulation (R3). Accordingly, although photosynthetic fixation (A1) is enhanced, benthic recycling processes (U1 and R3) are simultaneously intensified and partly offset the increase in net DIC consumption.

Therefore, the A/R response in the tidal-flat region constitutes a moderated regime in which pelagic uptake (A1) and benthic recycling processes (U1–R3) coexist.

7.4.2 Response of carbon fixation (F/U)

As shown in **Fig. 18(A)**, carbon fixation flux increases with increasing nutrient loading in the tidal-flat region. This increase is explained by the enhancement of pelagic primary production, corresponding to the nutrient-stimulated production pathway (F1) defined in **Sect. 6.2**.

However, as shown in **Fig. 19**, the seasonal dynamics of benthic fauna indicate that biomass does not increase monotonically throughout the year. Suspension feeders and deposit feeders increase during the spring–autumn growth period, whereas mortality increases during the summer hypoxic period, and the duration of this mortality period becomes longer under higher nutrient-loading conditions. These responses reflect the intensification of decomposition and oxygen-limitation-related loss processes, corresponding to remineralization-driven reduction (U1) and hypoxia-induced suppression (U2).

Accordingly, although fixation (F1) is enhanced, loss processes (U1–U2) are simultaneously intensified, and increases in fixation flux do not directly translate into proportional increases in biomass accumulation. Instead, production and loss processes are co-amplified.

Therefore, the F/U relationship in the tidal-flat region constitutes a transformation-dominated regime in which fixation-enhancement (F1–F3) is constrained by strong loss pathways (U1–U2).

7.4.3 Response of carbon storage (S/D)

As shown in **Fig. 19**, $CaCO_3$ storage in the tidal-flat region is maintained at a high level and exhibits the largest absolute amount among the three regions. This pattern reflects the persistence of carbonate-associated storage processes supported by large benthic-faunal biomass, shallow water depth, sufficient light penetration, and repeated emersion–inundation cycles that sustain oxygen supply to the benthic environment. These conditions correspond to the stabilisation of the carbonate-associated storage pathway (S2) defined in **Sect. 6.3**.

At the same time, organic matter supplied from the water column is rapidly processed within the benthic system through intensive decomposition and transformation processes. This behaviour reflects the dominance of transformation-driven pathways (S3), in which externally supplied organic carbon is not stored but continuously converted and remineralized.

https://doi.org/10.5194/egusphere-2026-2710
Preprint. Discussion started: 4 June 2026

Accordingly, although shell-forming supply (S2) is continuously maintained, organic-matter storage does not become the dominant component of sedimentary carbon storage due to the strong activity of transformation and decomposition processes (S3 and D1–D2).

Therefore, the S/D structure in the tidal-flat region constitutes a transformation-dominated regime, in which carbonate-associated storage (S2) is maintained, while organic carbon is continuously processed rather than accumulated.

7.4.4 Summary of the tidal-flat response

The tidal-flat region is summarised as follows:

- Uptake: a moderated amplification pattern, in which pelagic photosynthetic drawdown (A1) is enhanced but partially offset by benthic recycling processes (U1 and R3);
- Fixation: a transformation-dominated F/U structure, in which externally supplied organic matter is rapidly processed through remineralization and hypoxia-related loss pathways (U1–U2), limiting net biomass accumulation;
- Storage: a carbonate-associated storage structure, in which $CaCO_3$ accumulation (S2) is maintained, while organic carbon is continuously processed through transformation pathways (S3) and loss processes (D1–D2).

Accordingly, carbon dynamics in the tidal-flat region are governed less by new production than by transport, transformation, and redistribution within the benthic environment.

In contrast to the monotonic amplification regime of the estuarine region and the co-amplification regime of the central bay, the tidal-flat region constitutes a transformation-dominated regime governed by benthic processing and redistribution.

7.5 Comparison of control structures among the three regions

In this study, responses among the three regions are compared based on the dynamic framework of uptake (A/R), fixation (F/U), and storage (S/D) established in **Sect. 6**.

As shown in **Fig. 10**, a common tendency is observed in all three regions: both atmospheric CO_2 uptake and pelagic fixation increase with increasing nutrient loading. This shared response reflects the strengthening of supply-side processes, corresponding primarily to the pelagic photosynthetic drawdown (A1) and fixation pathways (F1–F2).

However, as revealed by the process-level decomposition analyses (**Figs. 11–19**), the relative relationships among the processes governing uptake, fixation, and storage differ systematically by region.

7.5.1 Estuarine region: monotonic amplification type

In the estuarine region, fixation-enhancement pathways (F1–F3) are amplified; reduction pathways (U1–U2) are also enhanced but do not exceed F; the F–U difference remains positive; and organic-matter storage (S1) increases, whereas carbonate-associated storage (S2) weakens.

https://doi.org/10.5194/egusphere-2026-2710
Preprint. Discussion started: 4 June 2026

Accordingly, amplification of supply-side processes is dominant, and no replacement of the control structure occurs. The estuarine response therefore constitutes a monotonic amplification regime, in which the existing structure is strengthened without structural transition.

7.5.2 Central bay region: co-amplification type

In the central bay region, fixation-enhancement pathways (F1–F3) increase sharply; reduction pathways (U1–U2) are simultaneously amplified; the F–U difference varies with nutrient loading; and both organic (S1) and carbonate (S2) storage increase.

Accordingly, both production and decomposition processes are strongly driven, resulting in a coupled amplification of supply-side and loss-side processes. Therefore, the central bay constitutes a co-amplification regime, in which production and decomposition are simultaneously intensified.

7.5.3 Tidal-flat region: transformation-dominated type

In the tidal-flat region, uptake (A1) increases, but amplification is moderated by benthic recycling (U1–R3); net fixation remains limited because of strong loss pathways (U1–U2); and carbonate-associated storage (S2) is maintained, while organic carbon is processed through transformation pathways (S3).

Accordingly, externally supplied organic matter is continuously transformed and remineralized within the benthic system. Therefore, the tidal-flat region constitutes a transformation-dominated regime, in which carbon circulates through transformation and redistribution rather than accumulation via new production.

7.5.4 Spatial differentiation of control structures

Thus, even under the same external forcing of increased nutrient loading, the estuarine region exhibits amplification of the existing structure, the central bay exhibits co-amplification of production and decomposition, and the tidal-flat region exhibits dominance of transformation processes.

Importantly, these differences do not simply reflect variations in flux magnitude but rather regional differences in the relative dominance of the processes governing A/R, F/U, and S/D. In other words, this study demonstrates that the expression of carbon-mitigation functions under nutrient enrichment is realised through spatially differentiated control structures.

This spatial divergence does not imply a discontinuous bifurcation; rather, it reflects a continuous modulation of the relative dominance of governing processes in response to nutrient loading. These regional characteristics are summarised in **Table 3**.

https://doi.org/10.5194/egusphere-2026-2710
Preprint. Discussion started: 4 June 2026

Table 3. Dual Carbon Loop matrix of carbon-control structures across the three regions.

Region	A/R Dominant Balance (Absorption)	F/U Dominant Balance (Fixation)	S/D Dominant Balance (Storage)	Structural Type
Estuarine region	A dominant amplification; limited R enhancement	F increases; F-U remains positive	Organic S dominant; weakened $CaCO_3$ contribution	Monotonic amplification
Central bay region	Concurrent A and R enhancement	F and U co-amplify; net balance load-dependent	Organic and $CaCO_3$ increase simultaneously	Co-amplification
Tidal-flat region	Moderate A increase; coupled regeneration	Transport-driven U relatively dominant	$CaCO_3$ dominant; stable S supply	Transformation-dominated

8 Synthesis: spatial differentiation of carbon-control structures in the Dual Carbon Loop

8.1 Integrated perspective of this study

Sect. 6 establishes the carbon-cycle structure in EMAGIN-B.C. ver.2 as a dual-loop system organised into three functional axes: uptake (A/R), fixation (F/U), and storage (S/D), each governed by dynamic imbalances between supply-side and loss-side fluxes across different temporal scales.

Sect. 7 compares responses in the estuarine, central bay, and tidal-flat regions based on this mechanistic framework. Across all three regions, increasing nutrient loading enhances atmospheric CO_2 uptake and pelagic carbon fixation, reflecting the strengthening of supply-side processes corresponding primarily to pelagic photosynthetic drawdown (A1) and fixation pathways (F1–F2).

However, the relative relationships among the processes governing uptake, fixation, and storage differ systematically among regions, as expressed by distinct combinations of governing pathways (A1–R3, F1–U2, and S1–S3).

Accordingly, these differences constitute the spatial differentiation of carbon-control structures. This perspective extends the Dual Carbon Loop framework by showing that carbon-cycle responses to nutrient enrichment are governed not only by flux magnitudes but also by the structural balance among uptake, fixation, and storage processes, as defined by the relative dominance of their underlying mechanisms.

8.2 Spatial differentiation of carbon-control structures

As summarised in **Table 3** (Dual Carbon Loop Control Structure Matrix), the three regions are categorised into distinct types based on the dominant balance relationships within A/R, F/U, and S/D. In the estuarine region, DIC consumption driven by

https://doi.org/10.5194/egusphere-2026-2710
Preprint. Discussion started: 4 June 2026

pelagic photosynthesis (A1, F1–F2) is dominant, and the existing control structure is strengthened, constituting a monotonic amplification regime. In the central bay, fixation-enhancement pathways (F1–F3) and reduction pathways (U1–U2) are simultaneously intensified, resulting in a co-amplification regime characterised by strong coupling between production and decomposition processes. In the tidal-flat region, externally supplied organic carbon is intensively processed through transformation pathways (S3) and remineralization processes (U1–U2), while carbonate-associated storage (S2) is stably maintained, constituting a transformation-dominated regime.

Thus, even under the same external forcing—namely increased nutrient loading—the carbon-mitigation function is not uniformly amplified; instead, it is realised through distinct control structures that emerge from region-specific balances among governing processes. Here, the term "control structure" refers to the relative dominance between supply-side and loss-side processes within each functional pair (A/R, F/U, S/D), as defined by the underlying mechanisms (A1–R3, F1–U2, and S1–S3). It does not imply a mathematical discontinuous bifurcation but rather a continuous modulation of process dominance in response to environmental forcing.

8.3 Nonlinearity and modulation of dominant balance

In the central bay, both fixation-enhancement pathways (F1–F3) and reduction pathways (U1–U2) are simultaneously intensified, resulting in a co-amplification structure. This structure reflects strong coupling between production and remineralization processes and demonstrates that the net balance between F and U is regulated by their relative intensities rather than by a unidirectional increase in production.

Although a clear discontinuous transition (bifurcation) is not identified, modulation of the dominant balance among governing pathways indicates structural conditions under which nonlinear responses may emerge. Accordingly, carbon cycling in coastal systems does not respond to increasing nutrient loading through a simple proportional relationship. Instead, system behaviour is governed by shifts in the relative dominance among internal ecosystem processes.

Thus, nonlinearity in coastal carbon cycling arises not from abrupt threshold behaviour but from continuous modulation of competing processes within the Dual Carbon Loop framework.

8.4 Implications for coastal carbon management

The results of this study indicate that carbon management in coastal systems cannot be evaluated solely based on changes in the magnitude of carbon uptake or fixation. Even under the same nutrient-control policy, distinct carbon-control structures govern system responses: pelagic amplification driven by photosynthetic pathways (A1, F1–F2) dominates in the estuarine region; production and decomposition pathways (F1–F3 and U1–U2) are simultaneously intensified in the central bay, resulting in a co-amplification structure; and transformation and redistribution processes (S3 and U1–U2) dominate in the tidal-flat region, while carbonate-associated storage (S2) is maintained. Accordingly, the evaluation and design of carbon-

https://doi.org/10.5194/egusphere-2026-2710
Preprint. Discussion started: 4 June 2026

mitigation strategies in coastal environments must explicitly account for region-specific carbon-control structures, rather than relying on uniform assumptions based solely on bulk carbon fluxes.

8.5 Conclusions

From the perspective of the Dual Carbon Loop, this study establishes an integrated framework for understanding the responses of carbon uptake, fixation, and storage to increased nutrient loading and demonstrates that their realization patterns are spatially differentiated.

Carbon cycling in urban coastal systems is not governed simply by quantitative changes in flux magnitude. Rather, diverse mitigation functions emerge from spatial differences in the relative dominance and arrangement of governing processes within the A/R, F/U, and S/D structures.

Accordingly, the concept of carbon-control structure proposed in this study provides a fundamental framework for process-based coastal ecosystem modelling and for the design of coastal carbon-management strategies.

Code and data availability

The EMAGIN-B.C. ver. 2 model code is an actively developed research code and is therefore not publicly deposited at this stage. The model code and processed model outputs used to generate the figures and tables in this study are available from the corresponding author upon reasonable request for academic and non-commercial purposes. Data derived from observational sources are subject to source-specific conditions.

Author contributions

K.K.: Formal analysis; Investigation; Software; Visualisation; Writing – original draft.

D.O.: Software; Model development.

A.S.: Conceptualisation; Methodology; Theoretical framework development; Model development; Funding acquisition; Supervision; Writing – original draft; Writing – review & editing.

Competing interests

The authors declare that they have no competing interests.

https://doi.org/10.5194/egusphere-2026-2710
Preprint. Discussion started: 4 June 2026

Acknowledgements

Part of this study is based on the Master's thesis research conducted by Kohei Kawahito under the supervision of Akio Sohma. The authors would like to thank all members of the Sohma Laboratory at Osaka Metropolitan University and former members at Osaka City University for their valuable discussions and support.

Financial support

This study was supported by the Japan Society for the Promotion of Science (JSPS) KAKENHI (Grant Numbers 18K04409 and 25H01449) and by the Environment Research and Technology Development Fund (JPMEERF24S12312) of the Environmental Restoration and Conservation Agency.
These grants were awarded to Akio Sohma (Principal Investigator for Grant 18K04409; Co-Investigator for Grants 25H01449 and JPMEERF24S12312).
The funders had no role in the decision to publish or in the preparation of the manuscript.

References

Alongi, D. M., Murdiyarso, D., Fourqurean, J. W., Kauffman, J. B., Hutahaean, A., Crooks, S., Lovelock, C. E., Howard, J., Herr, D., Fortes, M., Pidgeon, E., and Wagey, T.: Indonesia's blue carbon: A globally significant and vulnerable sink for seagrass and mangrove carbon, Wetl. Ecol. Manag., 24, 3–13, 2016.

Andersen, F. O.: Fate of organic carbon added as diatom cells to oxic and anoxic marine sediment microcosms, Mar. Ecol. Prog. Ser., 134, 225–233, 1996.

Ando, H., Yamazaki, M., and Soda, K.: Effects of acid rain on inland waters (Part 2), Annu. Rep. Tokyo Metrop. Res. Inst. Environ. Prot., 334–340, 1992, (in Japanese).

Archer, D. and Brovkin, V.: The millennial atmospheric lifetime of anthropogenic CO_2, Clim. Change, 90, 283–297, 2008.

Bastviken, D., Olsson, M., and Tranvik, L.: Simultaneous measurements of organic carbon mineralization and bacterial production in oxic and anoxic lake sediments, Microb. Ecol., 46, 73–82, 2003.

Butenschön, M., Clark, J., Aldridge, J. N., Allen, J. I., Artioli, Y., Blackford, J., Bruggeman, J., Cazenave, P., Ciavatta, S., Kay, S., Lessin, G., van Leeuwen, S., van der Molen, J., de Mora, L., Polimene, L., Sailley, S., Stephens, N., and Torres, R.: ERSEM 15.06: A generic model for marine biogeochemistry and the ecosystem dynamics of the lower trophic levels, Geosci. Model Dev., 9, 1293–1339, 2016.

Canfield, D. E.: Factors influencing organic carbon preservation in marine sediments, Chem. Geol., 114, 315–329, https://doi.org/10.1016/0009-2541(94)90061-2, 1994.

https://doi.org/10.5194/egusphere-2026-2710
Preprint. Discussion started: 4 June 2026

Chen, C.-T. A.: Air–sea exchanges of CO_2 in the world's coastal seas, Biogeosciences, 10, 6509–6544, 2013.

Chmura, G. L., Anisfeld, S. C., Cahoon, D. R., and Lynch, J. C.: Global carbon sequestration in tidal, saline wetland soils, Global Biogeochem. Cy., 17, 1111, https://doi.org/10.1029/2002GB001917, 2003.

Dickson, A. G., Sabine, C. L., and Christian, J. R.: Guide to best practices for ocean CO_2 measurements, North Pacific Marine Science Organization, 2007.

Donato, D. C., Kauffman, J. B., Murdiyarso, D., Kurnianto, S., Stidham, M., and Kanninen, M.: Mangroves among the most carbon-rich forests in the tropics, Nat. Geosci., 4, 293–297, 2011.

Falkowski, P., Scholes, R. J., Boyle, E., Canadell, J., Canfield, D., Elser, J., Gruber, N., Hibbard, K., Högberg, P., Linder, S., Mackenzie, F. T., Moore III, B., Pedersen, T., Rosenthal, Y., Seitzinger, S., Smetacek, V., and Steffen, W.: The global carbon cycle: A test of our knowledge of Earth as a system, Science, 290, 291–296, https://doi.org/10.1126/science.290.5490.291, 2000.

Fennel, K. and Wilkin, J.: Quantifying biological carbon export for the northwest North Atlantic continental shelves, Geophys. Res. Lett., 36, L18605, 2009.

Fourqurean, J. W., Duarte, C. M., Kennedy, H., Marbà, N., Holmer, M., Mateo, M. A., Apostolaki, E. T., Kendrick, G. A., Krause-Jensen, D., and McGlathery, K. J.: Seagrass ecosystems as a globally significant carbon stock, Nat. Geosci., 5, 505–509, 2012.

Frankignoulle, M., Abril, G., Borges, A. V., Bourge, I., Canon, C., Delille, B., Libert, E., and Théate, J.-M.: Carbon dioxide emission from European estuaries, Science, 282, 434–436, 1998.

Hedges, J. I. and Keil, R. G.: Sedimentary organic matter preservation: An assessment and speculative synthesis, Mar. Chem., 49, 81–115, 1995.

Hoffert, M. I., Wey, Y. C., Callegari, A. J., and Broecker, W. S.: Atmospheric response to deep-sea injections of fossil-fuel carbon dioxide, Clim. Change, 2, 53–68, 1979.

International EMECS Center (Ed.): Environmental conservation of the Seto Inland Sea, International EMECS Center, 2008.

IPCC, 2021: Climate Change 2021: The Physical Science Basis. Contribution of Working Group I to the Sixth Assessment Report of the Intergovernmental Panel on Climate Change, edited by Masson-Delmotte, V., Zhai, P., Pirani, A., Connors, S. L., Péan, C., Berger, S., Caud, N., Chen, Y., Goldfarb, L., Gomis, M. I., Huang, M., Leitzell, K., Lonnoy, E., Matthews, J. B. R., Maycock, T. K., Waterfield, T., Yelekçi, O., Yu, R., and Zhou, B., Cambridge University Press, Cambridge, UK and New York, NY, USA, 2391 pp., https://doi.org/10.1017/9781009157896, 2021.

Ishizuka, K. and Sohma, A.: A mechanistic model of hypoxia-driven benthic carbon cycling integrating microbial energetics and faunal mortality, EGUsphere [preprint], https://doi.org/10.5194/egusphere-2025-4822, 2025.

Japan Fisheries Engineering Association: Proposal for nutrient management strategies (On the necessity of nutrient management), 2024, (in Japanese).

https://doi.org/10.5194/egusphere-2026-2710
Preprint. Discussion started: 4 June 2026

Jessen, G. L., Lichtschlag, A., Ramette, A., Pantoja, S., Rossel, P. E., Schubert, C. J., Struck, U., and Boetius, A.: Hypoxia causes preservation of labile organic matter and changes seafloor microbial community composition (Black Sea), Sci. Adv., 3, e1601897, https://doi.org/10.1126/sciadv.1601897, 2017.

Kristensen, E. and Holmer, M.: Decomposition of plant materials in marine sediment exposed to different electron acceptors (O_2, NO_3^-, and SO_4^{2-}), with emphasis on substrate origin, degradation kinetics, and the role of bioturbation, Geochim. Cosmochim. Acta, 65, 419–433, 2001.

Kubo, A. and Kanda, J.: Seasonal variations and sources of sedimentary organic carbon in Tokyo Bay, Mar. Pollut. Bull., 114, 637–643, 2017.

Kuwae, T., Kanda, J., Kubo, A., Nakajima, F., Ogawa, H., Sohma, A., and Suzumura, M.: Blue carbon in human-dominated estuarine and shallow coastal systems, Ambio, 45, 290–301, 2016.

McLeod, E., Chmura, G. L., Bouillon, S., Salm, R., Björk, M., Duarte, C. M., Lovelock, C. E., Schlesinger, W. H., and Silliman, B. R.: A blueprint for blue carbon: Toward an improved understanding of the role of vegetated coastal habitats in sequestering CO_2, Front. Ecol. Environ., 9, 552–560, https://doi.org/10.1890/110004, 2011.

Ministry of Land, Infrastructure, Transport and Tourism: Guideline (Draft) for Effective Implementation of Active Operational Management of Nutrient Salts, Sewerage Department, Water and Disaster Management Bureau, Government of Japan, 2023, (in Japanese).

Ministry of the Environment: Guidance for Introducing the Total Pollutant Load Control System (TPLCS), Office of Environmental Management of Enclosed Coastal Seas, Water Environment Division, Environmental Management Bureau, Ministry of the Environment, Japan, April 2011, (in Japanese), 2011.

Murdiyarso, D., Purbopuspito, J., Kauffman, J. B., Warren, M. W., Sasmito, S. D., Donato, D. C., Manuri, S., Krisnawati, H., Taberima, S., and Kurnianto, S.: The potential of Indonesian mangrove forests for global climate change mitigation, Nat. Clim. Change, 5, 1089–1092, https://doi.org/10.1038/nclimate2734, 2015.

Nellemann, C., Corcoran, E., Duarte, C. M., Valdés, L., De Young, C., Fonseca, L., and Grimsditch, G. (Eds.): Blue Carbon: The Role of Healthy Oceans in Binding Carbon – A Rapid Response Assessment, UNEP/Earthprint, 78 pp., 2009.

Nishijima, W.: Development of methods for managing nutrient salt concentrations in the Seto Inland Sea (Enclosed coastal sea), Final Report of the Environmental Research and Technology Development Fund (S-13-1), 2014–2018, Hiroshima University and Kagawa University, 2019, (in Japanese).

Ogura, N. and Takada, H.: Tokyo Bay: 100 years of environmental change, Anzen Kogaku (J. Saf. Eng.), 34, 325–331, 1995, (in Japanese).

Ikuta, T., Kobayashi, H., Takahashi, M., Sase, H., Totsuka, T., and Satake, K.: A continuous water quality monitoring system to research the influence by acid rain in the Miomote-gawa River, Bull. JESC, 32, 48–53, 2005 (in Japanese).

Okamoto, S.: Development and dissemination of advanced treatment technologies contributing to water environment conservation, 50 Years of Water Environment in Japan, 63, 2021, (in Japanese).

https://doi.org/10.5194/egusphere-2026-2710
Preprint. Discussion started: 4 June 2026

Omachi, K. and Sohma, A.: Influence of marine organisms' pH dependency on carbon uptake, capture, and storage functions, J. Jpn. Soc. Civ. Eng., Ser. B2 (Coast. Eng.), 78(2), I_901–I_906, 2022, https://doi.org/10.2208/kaigan.78.2_I_901, (in Japanese with English abstract).

Omachi, K. and Sohma, A.: Future prediction of climate change mitigation functions in Tokyo Bay: An analysis using a coastal ecosystem model considering the effects of ocean acidification, J. Jpn. Soc. Civ. Eng., 79, 23-17154, 2023, https://doi.org/10.2208/jscejj.23-17154, (in Japanese with English abstract).

Sohma, A., Shibuki, H., Nakajima, H., Kubo, A., and Kuwae, T.: Modeling a coastal ecosystem to estimate climate change mitigation and a model demonstration in Tokyo Bay, Ecol. Model., 384, 261–289, 2018.

Solomon, S.: Climate Change 2007: The Physical Science Basis, Contribution of Working Group I to the Fourth Assessment Report of the Intergovernmental Panel on Climate Change, Cambridge University Press, 2007.

Thomas, H., Schiettecatte, L.-S., Suykens, K., Koné, Y. J. M., Shadwick, E. H., Prowe, A. E. F., Bozec, Y., de Baar, H. J. W., and Borges, A. V.: Enhanced ocean carbon storage from anaerobic alkalinity generation in coastal sediments, Biogeosciences, 6, 267–274, https://doi.org/10.5194/bg-6-267-2009, 2009.

Thomsen, J., Ramesh, K., Sanders, T., Bleich, M., and Melzner, F.: Calcification in a marginal sea – influence of seawater [Ca^{2+}] and carbonate chemistry on bivalve shell formation, Biogeosciences, 15, 1469–1482, 2018.

Turi, G., Lachkar, Z., and Gruber, N.: Spatiotemporal variability and drivers of pCO_2 and air–sea CO_2 fluxes in the California Current System: An eddy-resolving modeling study, Biogeosciences, 11, 671–690, 2014.

Wanninkhof, R.: Relationship between wind speed and gas exchange over the ocean revisited, Limnol. Oceanogr. Methods, 12, 351–362, https://doi.org/10.4319/lom.2014.12.351, 2014.

Yakushev, E. V., Protsenko, E. A., Bruggeman, J., Wallhead, P., Pakhomova, S. V., Yakubov, S. Kh., Bellerby, R. G. J., and Couture, R.-M.: Bottom RedOx Model (BROM v.1.1): A coupled benthic–pelagic model for simulation of water and sediment biogeochemistry, Geosci. Model Dev., 10, 453–482, https://doi.org/10.5194/gmd-10-453-2017, 2017.

Yates, K. K., Dufore, C., Smiley, N., Jackson, C., and Halley, R. B.: Diurnal variation of oxygen and carbonate system parameters in Tampa Bay and Florida Bay, Mar. Chem., 104, 110–124, https://doi.org/10.1016/j.marchem.2006.12.008, 2007.

Zhou, X., Li, H., Liang, J., Liu, H., Wang, X., Gao, L., Chen, L., Li, Y., Guo, Y., and Liang, S.: The role of marine bivalves in the oceanic carbon cycle: Physiological processes, carbon budgets and ecosystem perspectives, Reg. Stud. Mar. Sci., 78, 103815, 2024.